Molecular dynamics simulations of nuclear waste glasses and their aqueous corrosion behaviors

Jincheng Du

Department of Materials Science and Engineering, University of North Texas, Denton, Texas, USA

UNT UNIVERSITY OF NORTH TEXAS EST. 1890

Nimes, France

Sept. 25-29, 2023

sumglass
September 25–29th 2023
3rd Summer School on nuclear and industrial glasses for energy transition

Advances in understanding glass corrosion

- Glass corrosion is a complex process with coupled interfacial reactions and ion transport behaviors.
- For nuclear waste glasses, the complexity of composition and glass structure further complicated the problem.
- Various experimental techniques have been used to study glass corrosion: NMR, SIMS, XPS, SEM/TEM, APT, SHG.
- Simulations have also been applied to investigate glass corrosion: MD, MC, AIMD, machine learning approaches.

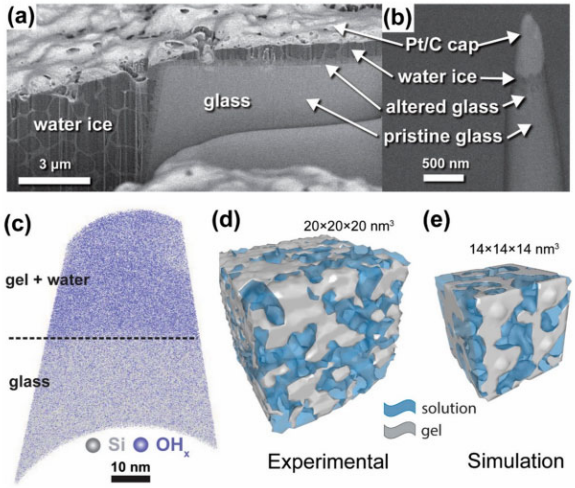

APT of gel layer

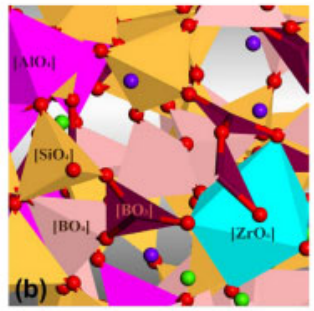

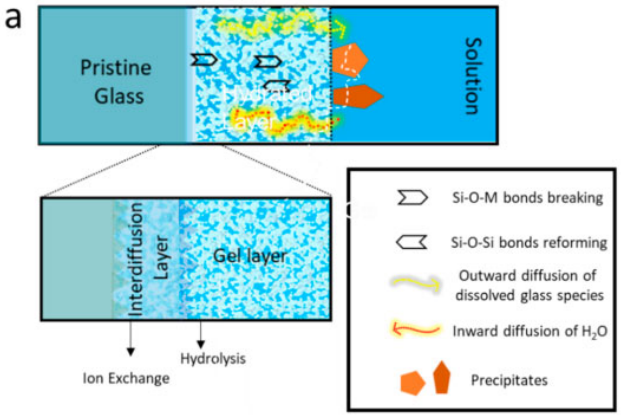

Frankel et al. Chem. Rev. 121(2021)12327

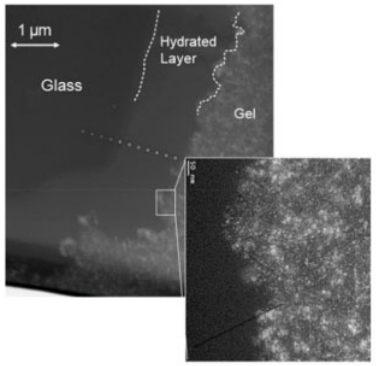

SEM image of interface

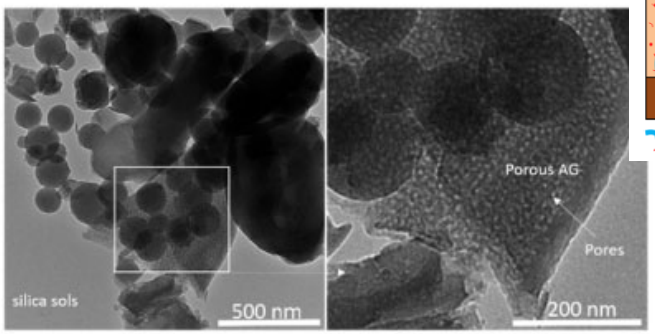

TEM image of gel layer

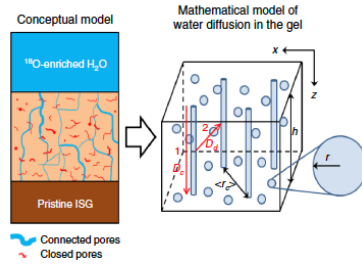

Gin et al. Nature Comm. 9(2018)2169

What can MD simulations contribute to understand glass corrosion?

- Obtain accurate atomic structural models of multicomponent nuclear waste glasses
- Calculate diffusion rate and energy barriers: cations, anions and water molecules

- Determine energy barriers for particular reactions (ion exchange, hydrolysis etc.)
- Identifying reaction mechanisms: ion exchange, hydrolysis, water transport etc.

- Gel layer formation and water/ion transport
- Glass surface morphology evolutions

- ML and MD based QSPR analysis of corrosion rate
- Monte Carlo simulations with glass structure model from MD simulations

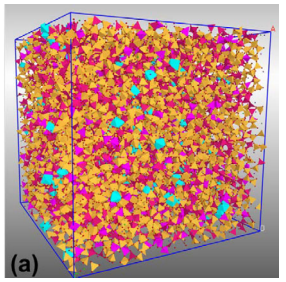

Gin et al. Nature Comm. 2018

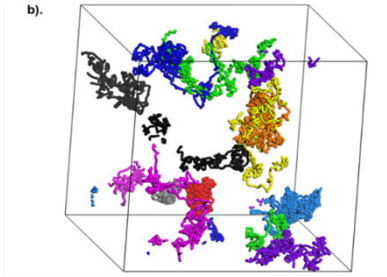

Rimsza, Du, JPCC 2017

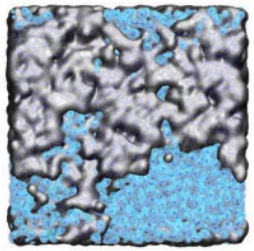

Mahadevan, Du, JNCS 2023

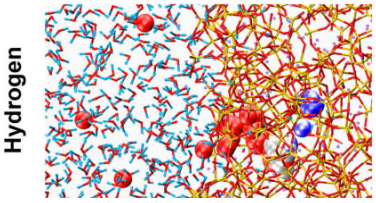

Deng et al. npj Mater Degr. 2019

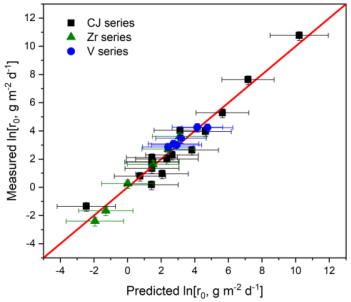

Lu et al. JACerS 106(2022)1025

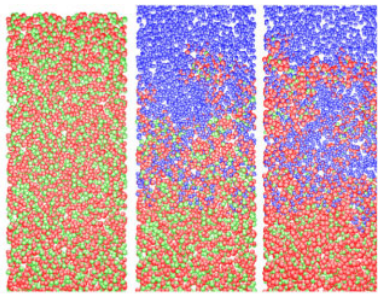

Kerisit, Du JNCS 522(2019)119601

Computer simulation methods

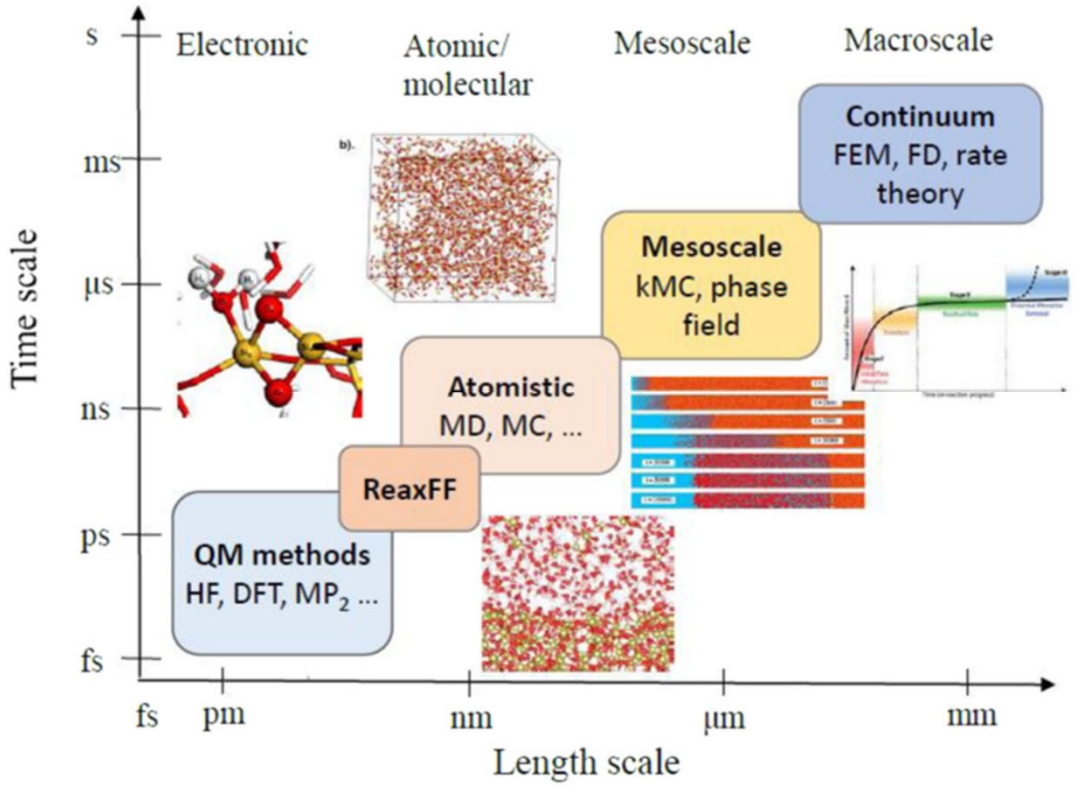

Du and Rimsza, NPJ Mater. Degrad. 1(2017)6

Quantum Mechanical method:

$$[\frac{-\hbar^2}{2m}\nabla^2+V]\Psi=i\hbar\frac{\partial}{\partial t}\Psi$$

Molecular Dynamic method:

$$\boldsymbol{f_i = m_i\ddot{r}_i = m_i\frac{\partial^2 r_i}{\partial t^2}}$$

Monte Carlo method:

$$p=\exp(-\Delta E/kT)$$

Rate theory:

$$r_2 = k_+(H^+)^n e^{\frac{-E_a}{RT}}\left(1-\frac{Q}{K}\right)$$

Fundamental Understanding of Glass Corrosion from atomistic simulations

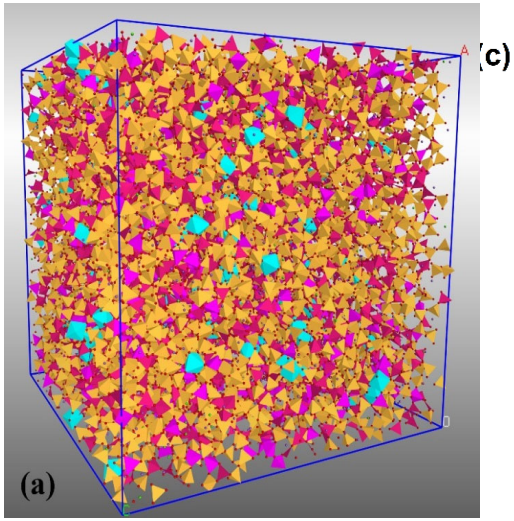

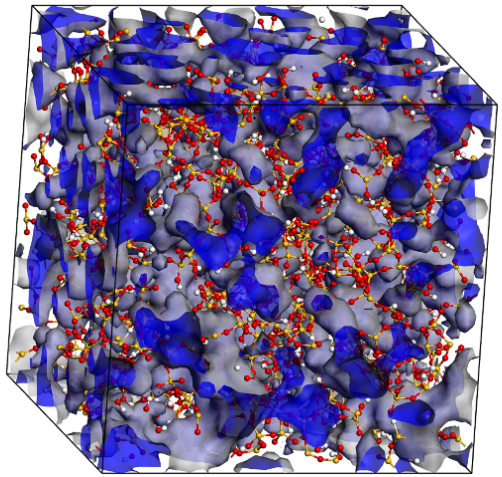

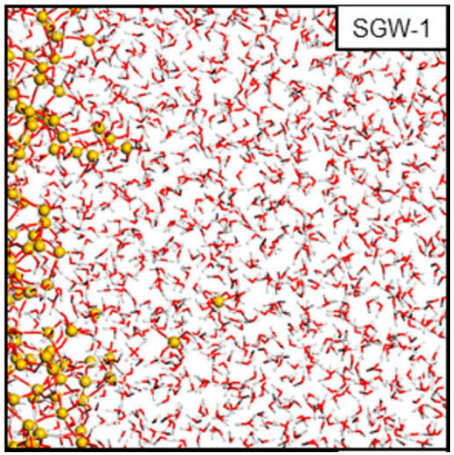

Glass structure models → Gel structure and water diffusion → Interfacial structure and evolution

Multicomponent glass dissolution mechanism & rate predictions

MD simulation of glass formation

Melt at 5000 K

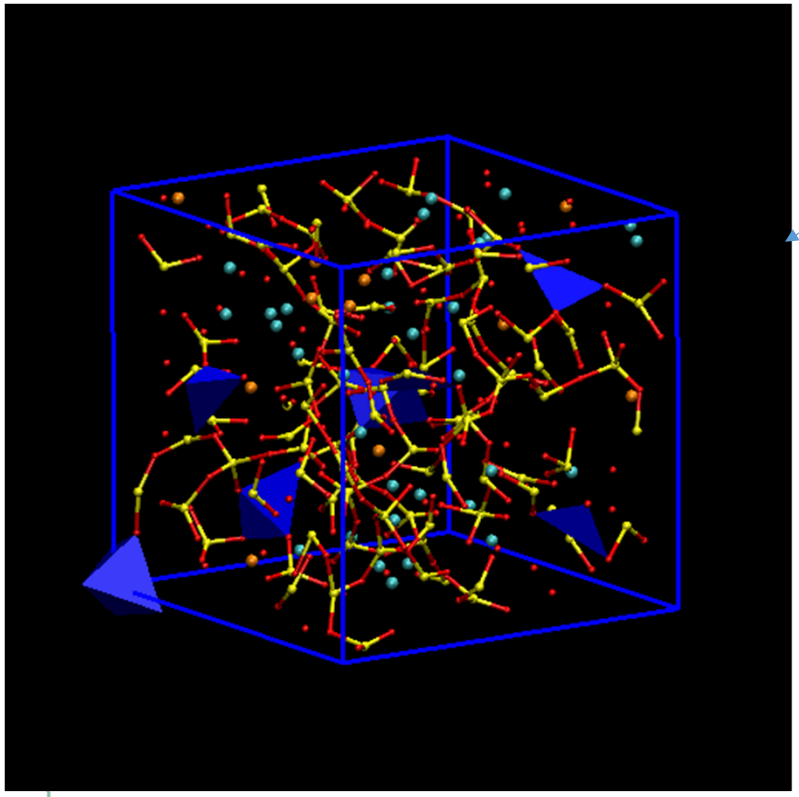

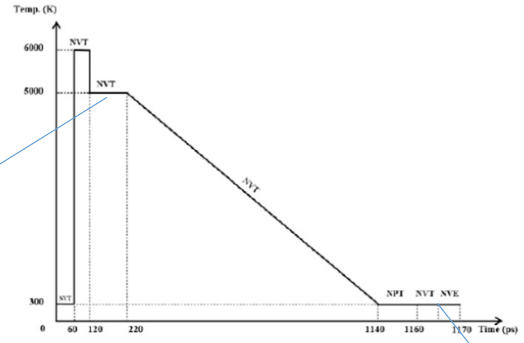

Glass at 300 K

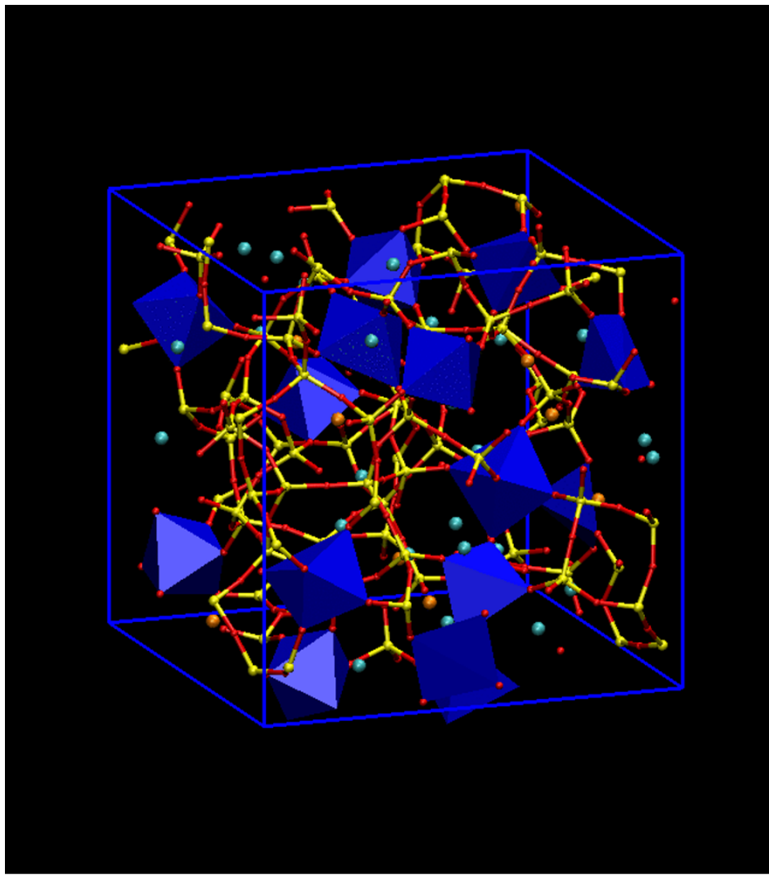

Red: O
Yellow: Si
Green: Na
Pink: Ca
Blue polyhedral: [ZrO_6]

MD simulation of a ZrO_2 containing soda lime silicate glass. (Lu et al., JNCS 2018)

Potential development for multicomponent borosilicate glasses

$$V(r_{ij}) = \frac{Z_i Z_j e^2}{4\pi\varepsilon_0 r_{ij}} + A_{ij}\exp(-r_{ij}/\rho_{ij}) - C_{ij}/r_{ij}^6$$

$$V'(r_{ij}) = B_{ij}/r_{ij}^n + D_{ij}\cdot r_{ij}^2$$

Du and Cormack, J. Am. Ceram. Soc. 88(2005)2532
Du and Corrales, JNCS 352(2006)3255
Du et al. , J. Am. Ceram. Soc. 94(2011)2393

$$A_{B-O} = \begin{cases} A_1 + t_1 \times (R_{max} - (R_{max} - N_4)^2/R_{max}) + t_2 \times K^2 & R \le R_{max} \\ A_2 + t_3 \times R_{max} \times N_4/R & R \ge R_{max} \end{cases}$$

$$t_3 = (A_1 + t_2 \times K^2 - A_2/R_{max} + t_1)$$

Variable	A_1(eV)	A_2(eV)	t_1(eV)	t_2(eV)
Parameter	11900.00	12525.00	4350.00	85.00

Lu et al. J. Phys. Chem. B. 122(2018)2564
Lu, Deng, Sebastien, Du, NPJ Mater. Degarad. 2(2018)19
Deng and Du, J. Am. Ceram. Soc. 102(2019)2482

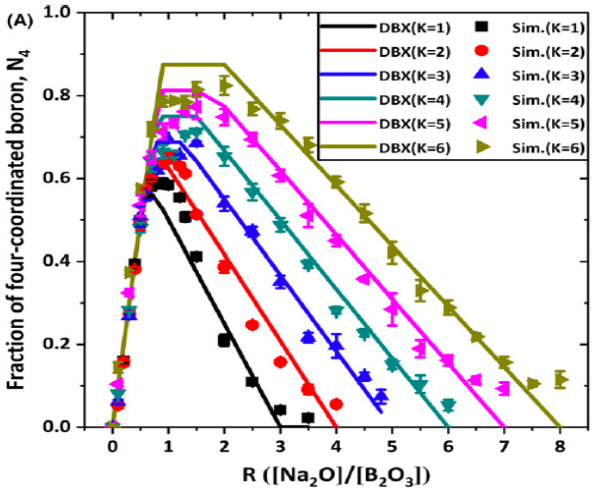

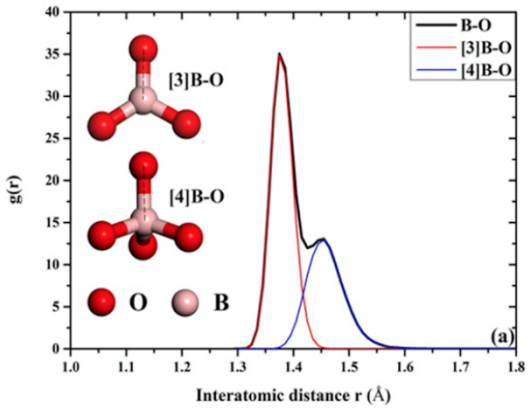

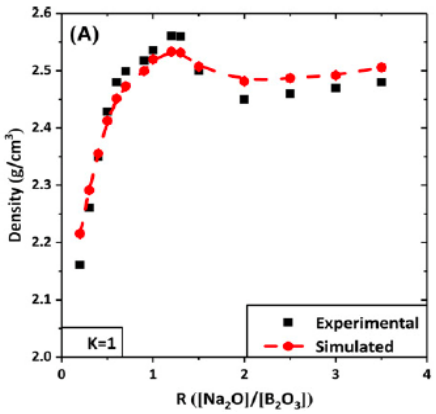

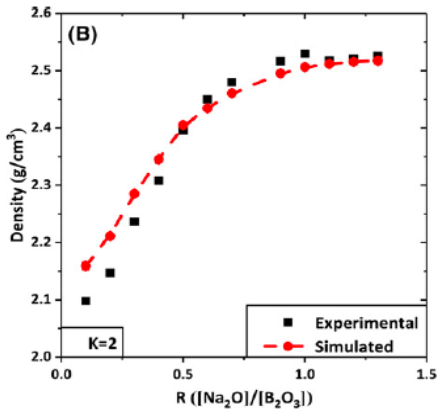

ISG Structures from MD: experimental validations

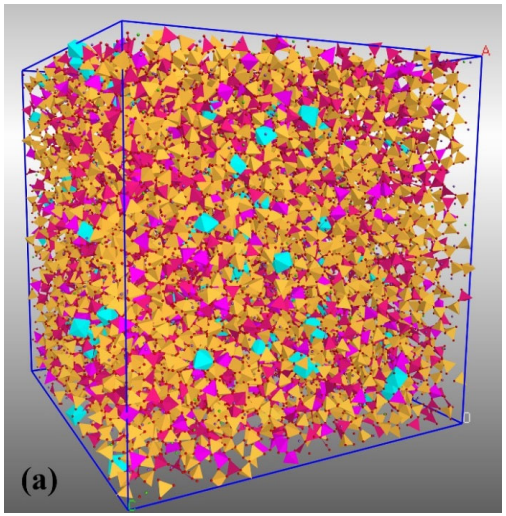

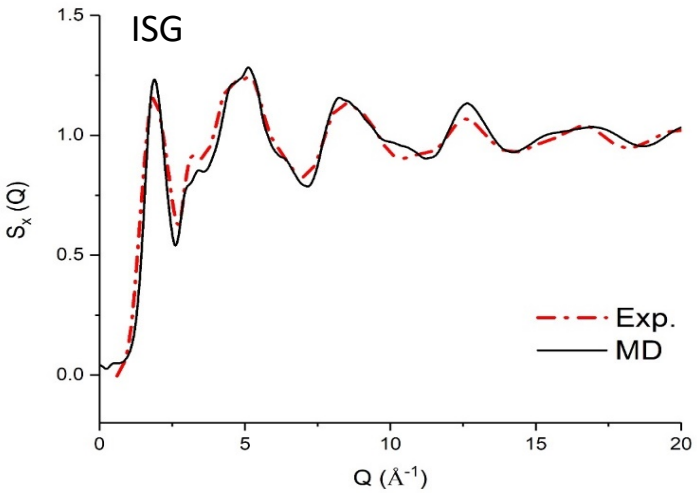

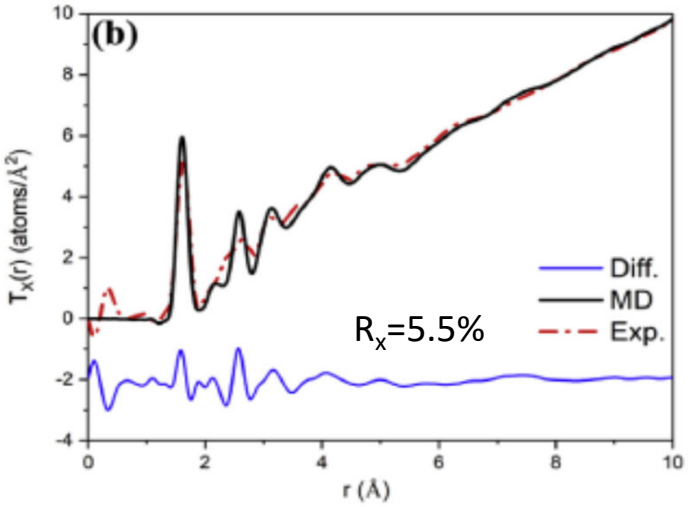

(mol%)	SiO_2	Al_2O_3	B_2O_3	CaO	Na_2O	ZrO_2
ISG*	60.2	3.8	16.0	5.7	12.6	1.7

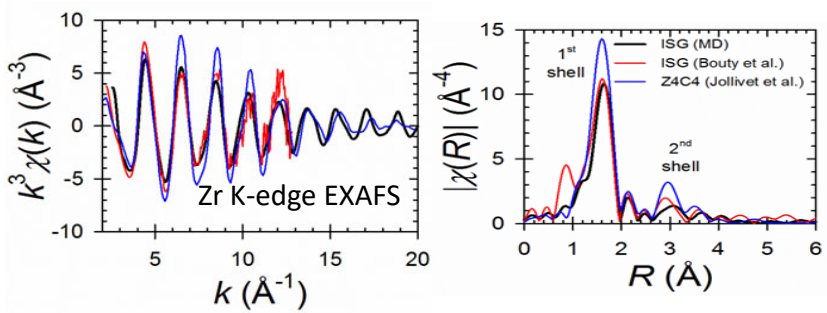

** Gin et al. Materials Today, 16(2013)243*

M. Collin et al., npj Materials Degradation. 2018;2:4.
X. Lu, L. Deng, S. Kerisit, J. Du, npj Materials Degradation, 2018; 2:19
X. Lu, L. Deng, C. Benmore, J. Du, J. Nuclear Mater. 515(2019)284

UNT UNIVERSITY OF NORTH TEXAS EST. 1890

ISG glass general structure features

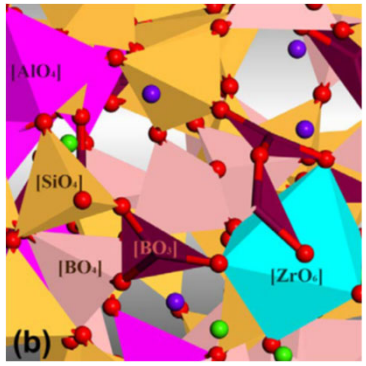

X	r_{X-O} (Å)	r_{cut}(Å)	$CN_{avg.}$	Coordination Number (CN) (%)				
				3	4	5	6	7
Si	1.61	2.25	**4.00**	--	100	--	--	--
B	1.45 ($^{[3]}$B) 1.55 ($^{[4]}$B)	2.00	**3.59**	41.3	58.7	--	--	--
Al	1.77	2.25	**4.00**	0.5	98.6	0.9	--	--
Zr	2.10	2.85	**5.68**	--	--	10.7	85.7	3.6

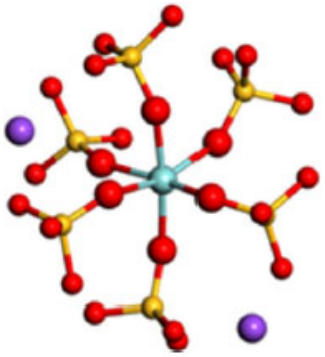

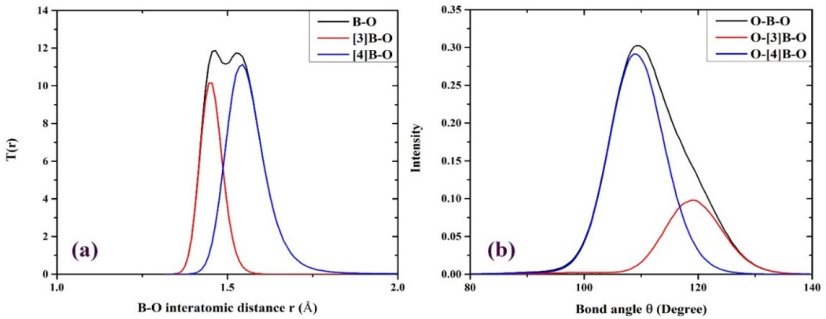

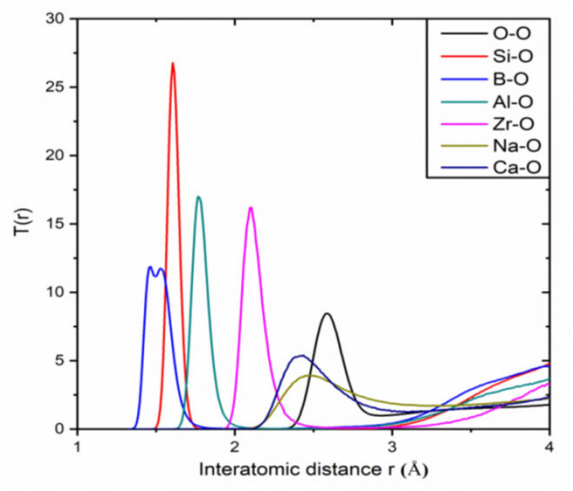

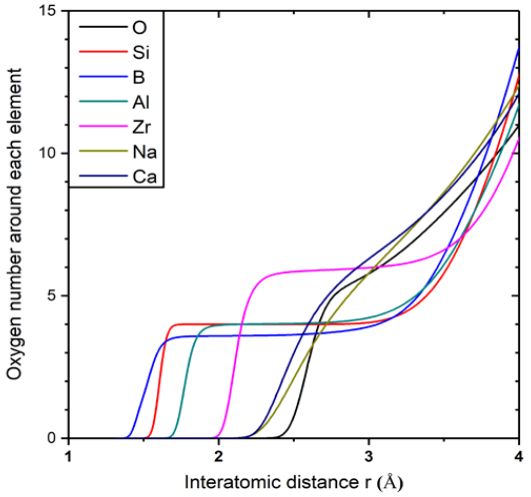

Collin et al. NPJ Mater. Degrad. 2(2018)

MD simulations of iron redox ratio effect

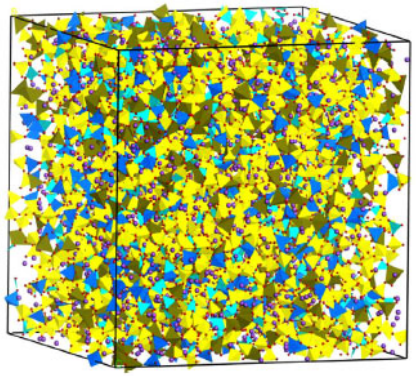

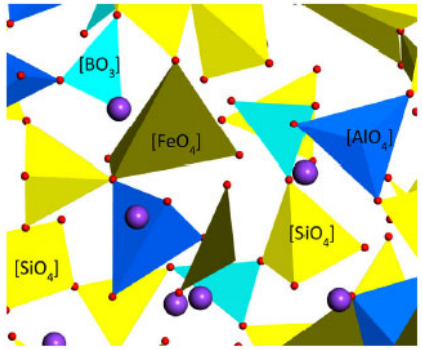

- Iron redox ratio effect on the structure of sodium silicate & boroaluminosilicate glasses
- Fe^{3+} plays the role of former while Fe^{2+} plays the role of modifier
- Reduction of iron, lead to an increase of boron N_4 values

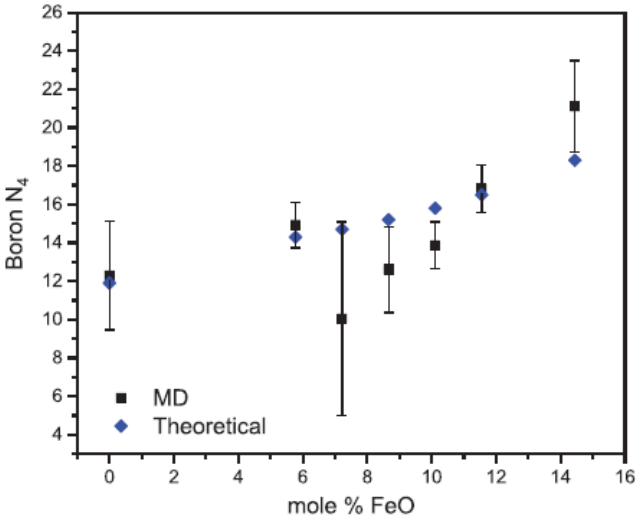

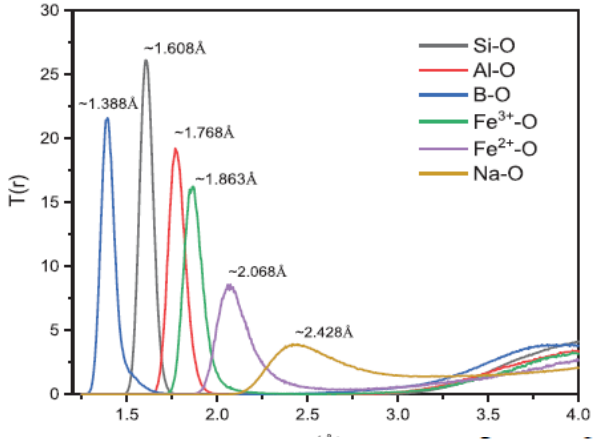

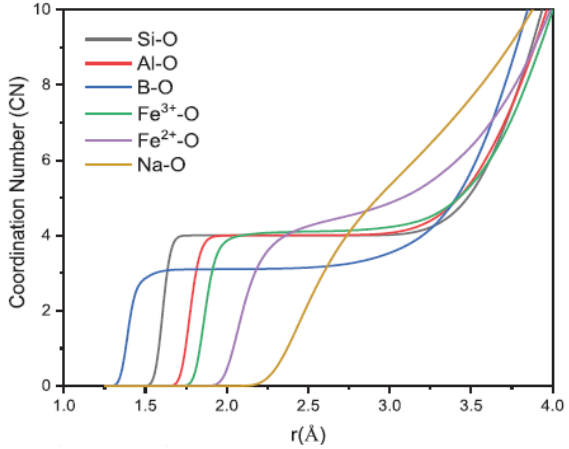

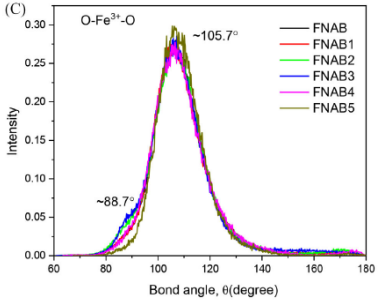

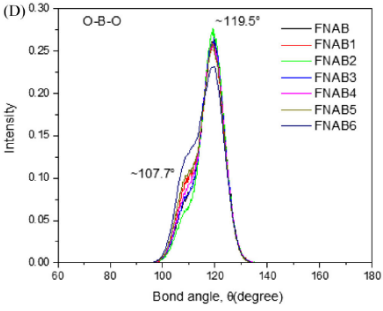

$$53.32SiO_2–9.12B_2O_3–23.93Na_2O–6.40Al_2O_3–(7.22 – x)Fe_2O_3–2xFeO\ (mol\%)$$

Tuheen, Sun, Du, JACerS, 2022
Nienhuis, Tuheen, Du, McCloy, J Mater Sci. 2021
Balasubramanya, Tuheen, .., Du, Goel, in prep.

Phase separation in glasses from MD simulations

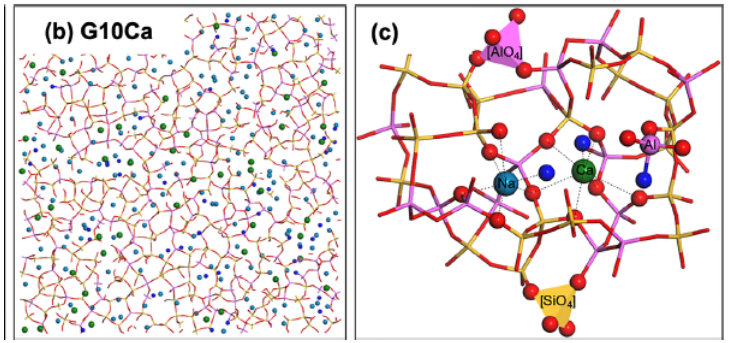

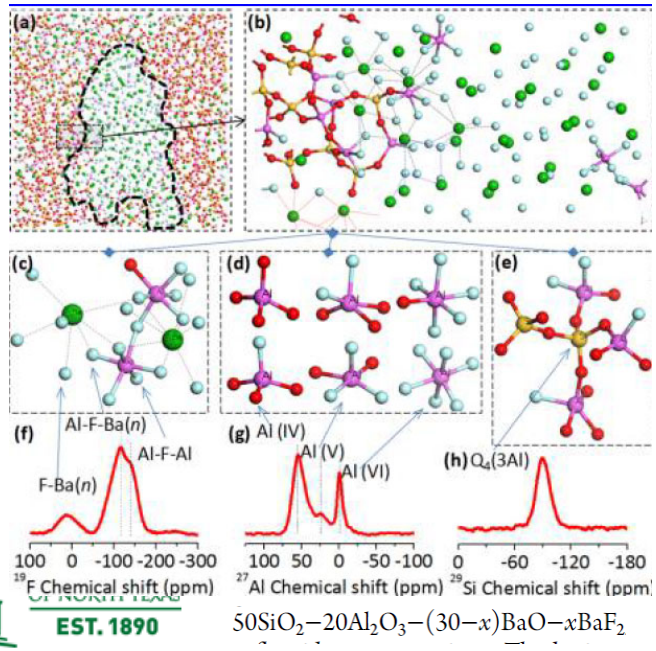

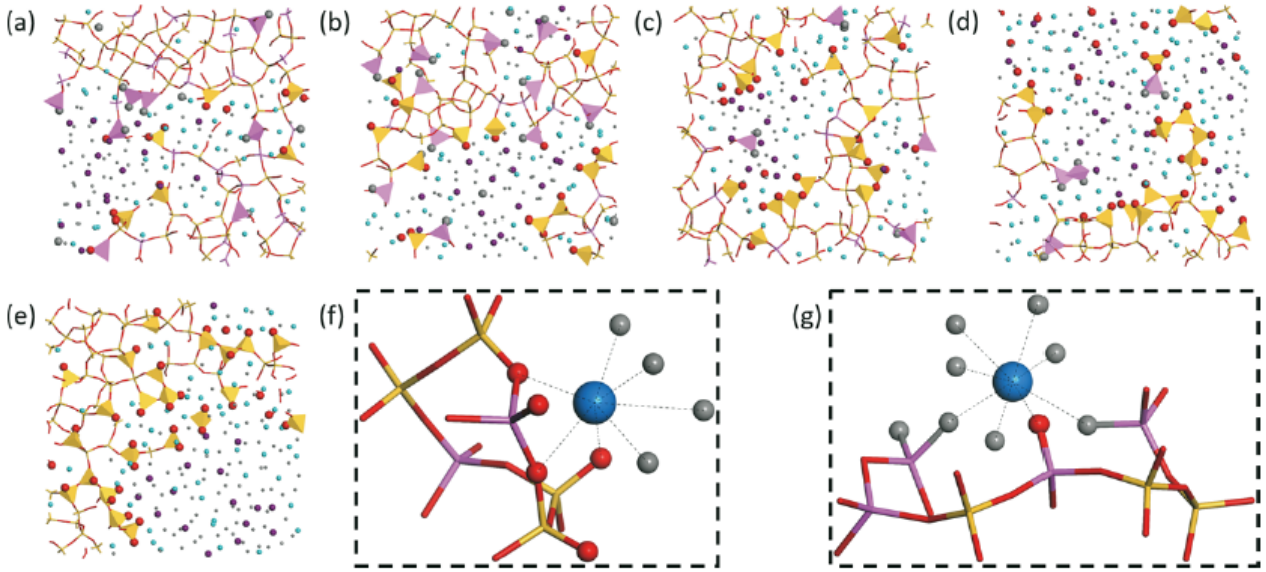

- MD simulations of fluorosilicate glasses with CaO/Na_2O substitution lead to more Ca-F bonds that helps of F retention in waste glasses
- Barium aluminosilicate oxyfluoride glass show phase separation in certain fluoride concentration
- La^{3+} were studied in oxyfluoride glasses and found to preferentially exist in the fluoride region

Zhao, Nienhuis, McCloy, Du, JNCS 2020
Zhao et al, J Phys Chem. B 2016
Zhao et al., J. Phys Chem B, 2020

Potentials can handle reactions: Reactive Force Field

$$E_{\text{potential}} = \left(E_{\text{bond}} + E_{\text{over}} + E_{\text{under}}\right) + \left(E_{\text{valency angle}} + E_{\text{penalty}}\right) + E_{\text{torsion}}$$

$$+ E_{\text{lone pair}} + E_{\text{conjugation}} + E_{\text{H-bond}} + E_{\text{vdWaals}} + E_{\text{Coulomb}}$$

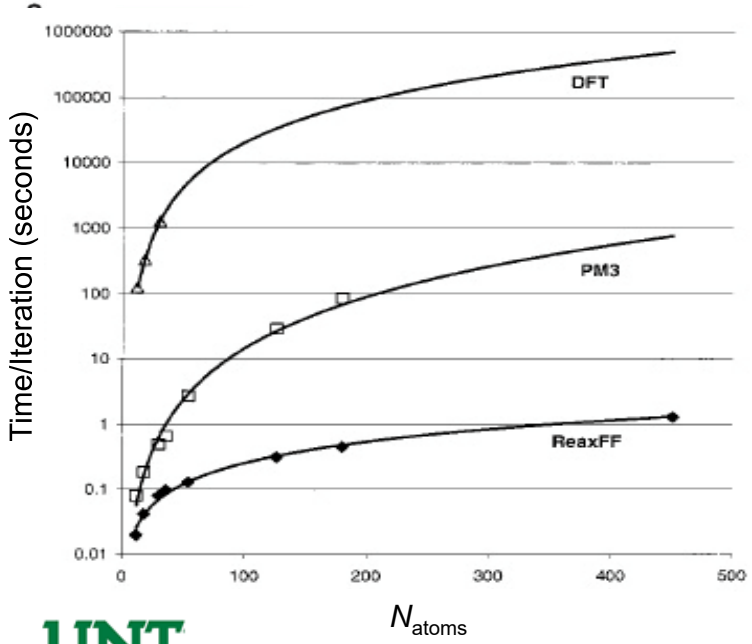

Bond order calculations:

$$BO'_{ij} = \exp\left[p_{bo,1}\cdot\left(\frac{r_{ij}}{r_o^{\sigma}}\right)^{p_{bo,2}}\right] + \exp\left[p_{bo,3}\cdot\left(\frac{r_{ij}}{r_o^{\pi}}\right)^{p_{bo,4}}\right] + \exp\left[p_{bo,5}\cdot\left(\frac{r_{ij}}{r_o^{\pi\pi}}\right)^{p_{bo,6}}\right]$$

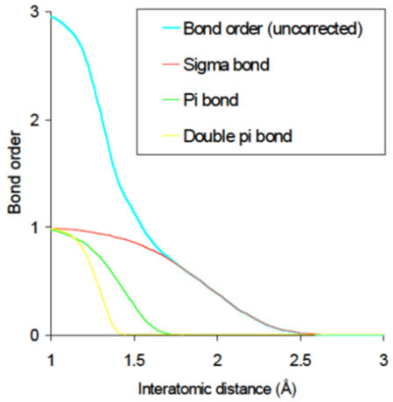

$$E_{\text{bond}} = -D_{\text{e}}\cdot \text{BO}_{ij}\cdot\exp\left[p_{\text{be},1}\left(1-\text{BO}_{ij}^{p_{\text{be},1}}\right)\right]$$

Charge calculations: Electronegativity Equalization Method (EEM: Mortier, et al, *JACS*, 108, 4315, ('86).) to calculate the charge equilibration

$$E = \sum_{i<j}\frac{q_i q_j}{r_{ij}} + \sum_i\left(\chi_i q_i + \tfrac{1}{2}J_i q_i^2\right) \qquad E_{\text{Coulomb}} = C\cdot\frac{q_i\cdot q_j}{\left[r_{ij}^3 + (1/\gamma_{ij})^3\right]^{1/3}}$$

Diffuse Charge Reactive Potential (DCRP)

2-body interactions

$$E_{2body} = E_{qq} + E_{q^d q^d} + E_{qq^d} + E_{q^d q} + E_{rep} + E_{disp}$$

where

$$E_{qq} = \frac{q_i q_j}{r_{ij}} \operatorname{erfc}\left(\frac{r_{ij}}{\beta}\right)$$

$$E_{qq^d} = E_{q^d q} = \frac{q_i q_j}{4 r_{ij}} \operatorname{erf}\left(\frac{r_{ij}}{\sqrt{2}\,\xi_{ij}}\right) \operatorname{erfc}\left(\frac{r_{ij}}{\beta}\right)$$

$$E_{q^d q^d} = \frac{q_i q_j}{16 r_{ij}} \operatorname{erfc}\left(\frac{r_{ij}}{2\xi_{ij}}\right) \operatorname{erfc}\left(\frac{r_{ij}}{\beta}\right)$$

$$E_{rep} = A_{rep}^{ij} \frac{\operatorname{erfc}(z_{ij})}{z_{ij}} \qquad \left[\text{with } z_{ij} = \frac{r_{ij}}{2\xi_{ij}}\right]$$

$$E_{disp} = \frac{-C_6^{ij}}{r_{ij}^6}$$

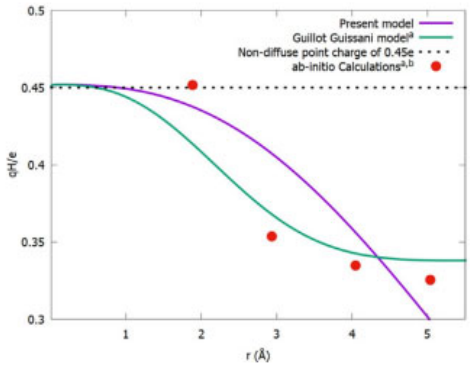

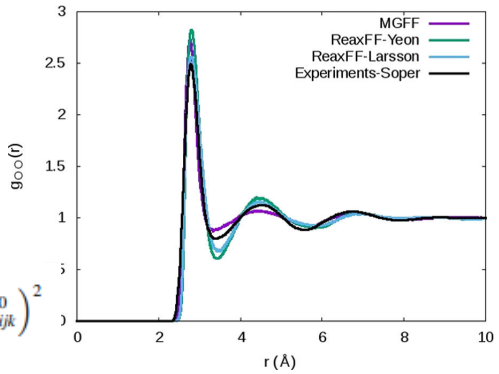

3-body interactions

$$U_{ijk}^{thr} = \lambda_{ijk} exp\left(\frac{\gamma_{ij}}{r_{ij} - r_{ij}^0} + \frac{\gamma_{ik}}{r_{ik} - r_{ik}^0}\right)\left(cos\theta_{ijk} - cos\theta_{ijk}^0\right)^2$$

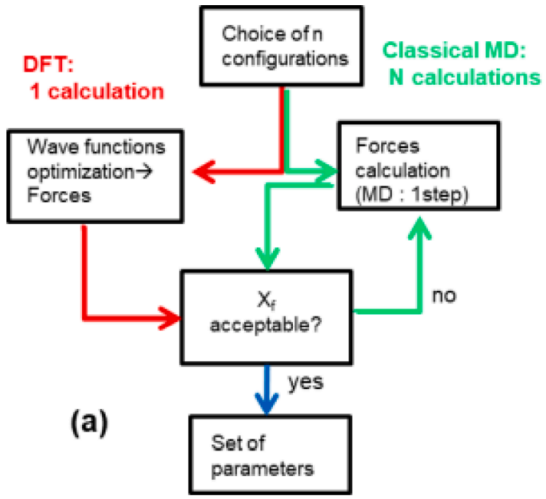

- Dissociable water potential obtained by force matching of AIMD results.
- Can describe reactions as well as physical properties of water
- Originally for water-silica system and recently added Na, Ca, Al to the potential sets
- It has advantage of speed (~10x faster than ReaxFF)

Mahadevan, Garofalini, J. Phys. Chem. C 112(2008)1507
Mahadevan, Wei, Du, J. Am. Ceram. Soc. 103(2020)3676
Mahadevan et al. J. Non-Cryst. Solids, 592(2022)121764

UNT UNIVERSITY OF NORTH TEXAS EST. 1890

Sodium silicate glass-water reactions

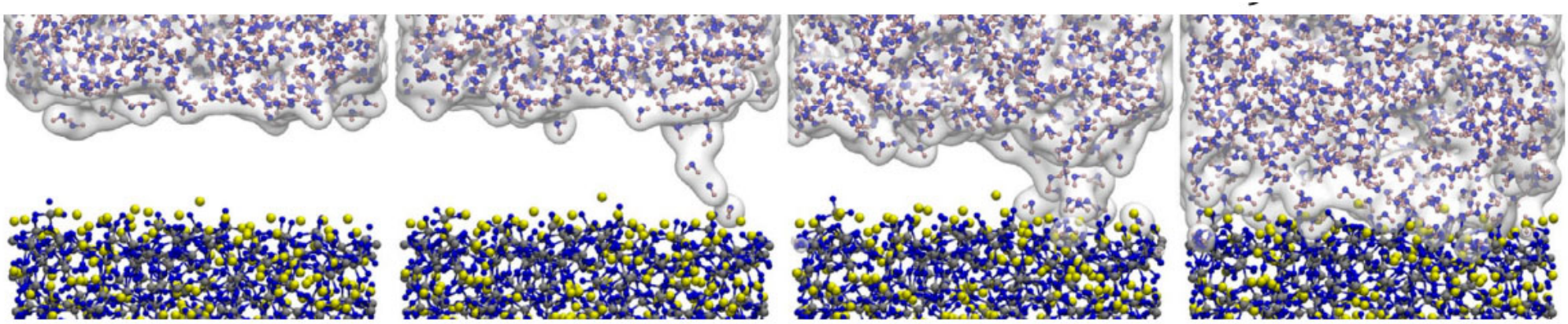

$30Na_2O$-$70SiO_2$

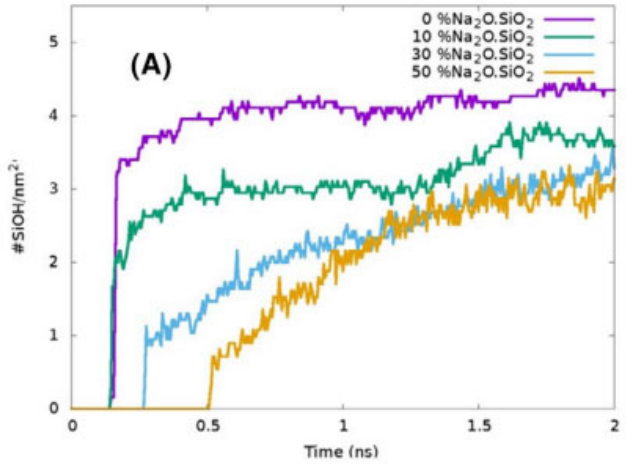

- Silica and a series xNa_2O-$(100-x)SiO_2$ (x=10-50) glasses were modeled using the DCRP potential
- Glass composition has a strong effect on initial glass-water interaction, or wetting of the glass surface

Mahadevan and Du, J. Am. Ceram. Soc. 103(2020)3676

Na silicate glass-water reactions: glass composition effect

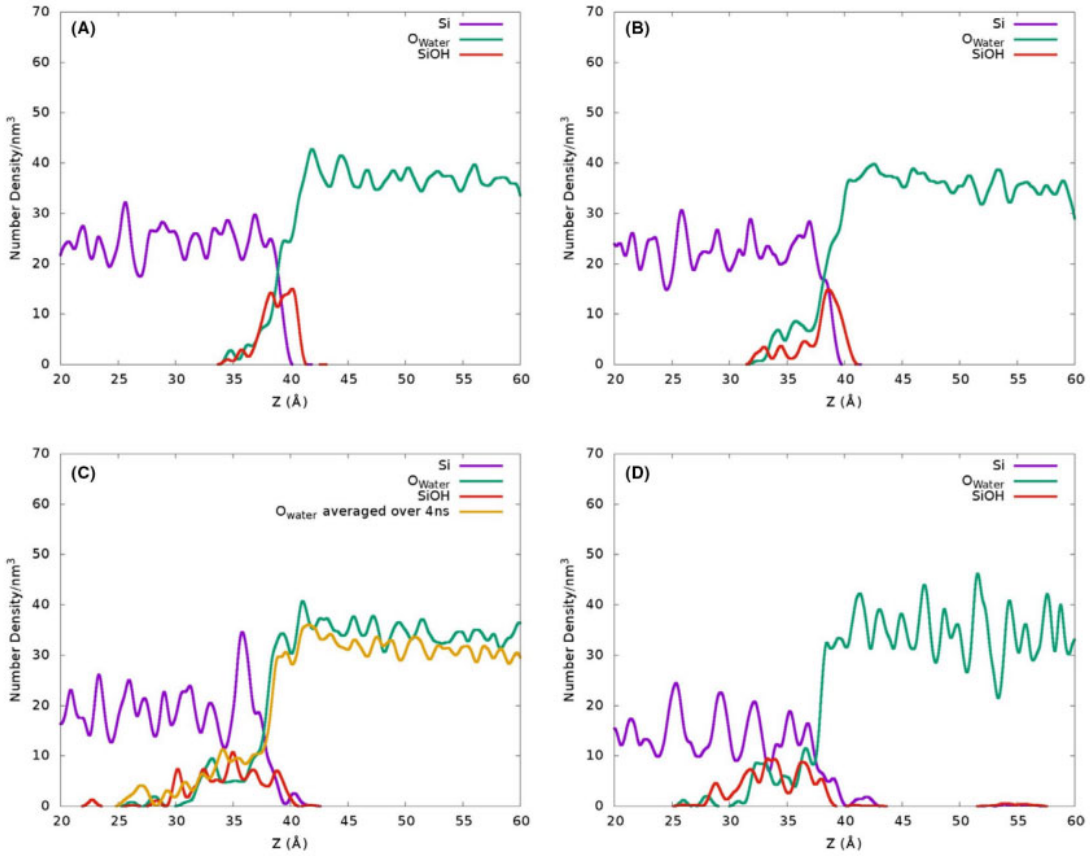

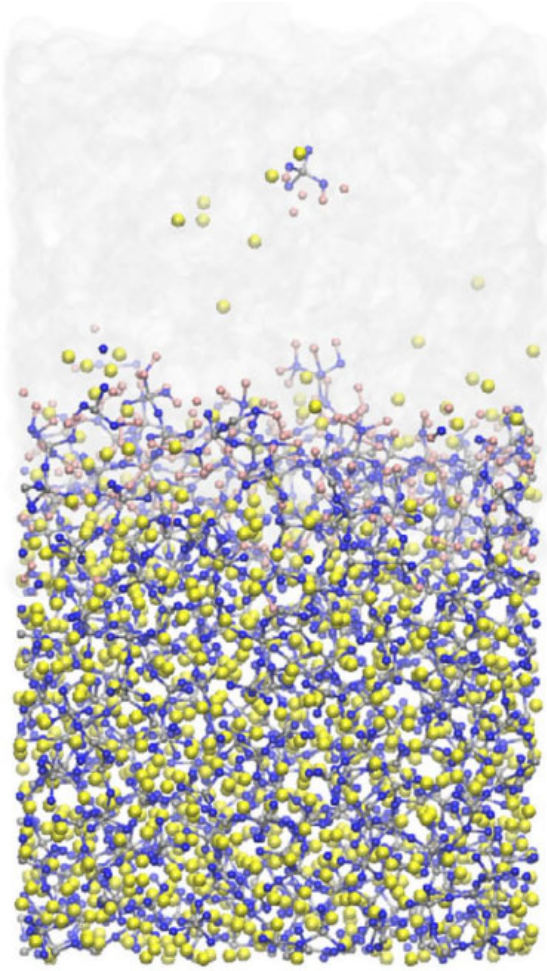

$30Na_2O$-$70SiO_2$ glass-water reaction, 300K, DCRP potential

Mahadevan and Du, J. Am. Ceram. Soc. 103(2020)3676

Sodium silicate glass - water reactions from reactive MD simulations

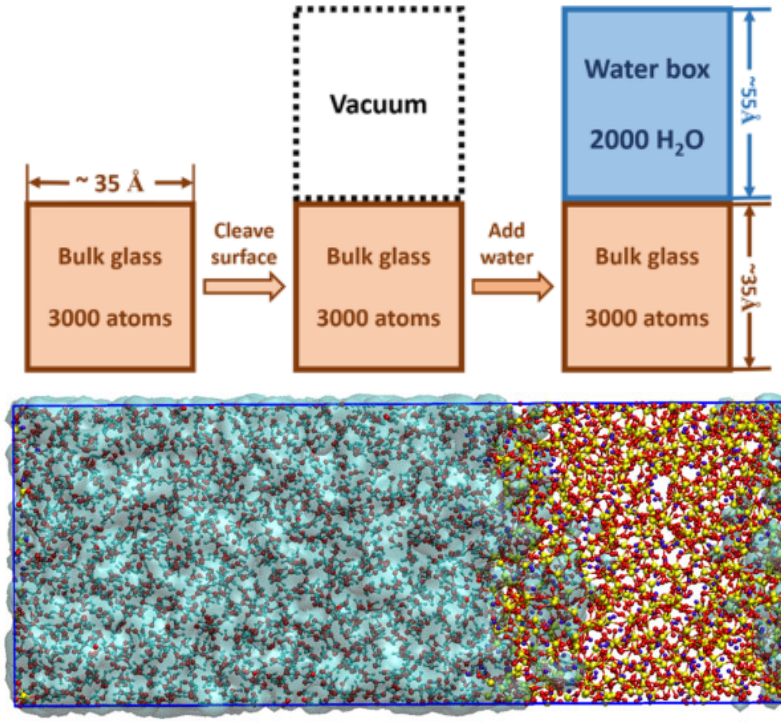

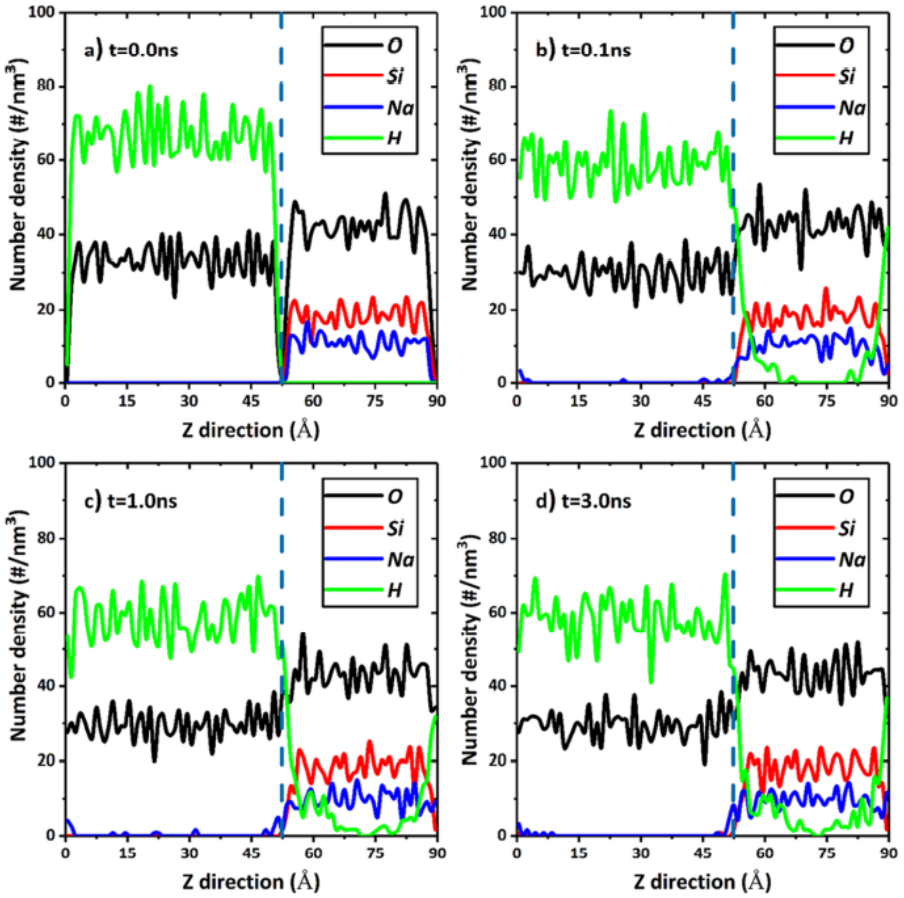

- ReaxFF based MD simulations up to 3 ns
- $77SiO_2$-$23Na_2O$ glass
- Four temperatures studied

Hahn et al. J. Phys. Chem. 122(2018)19613

Deng et al. J. Phys. Chem. 123(2019)21538

Sodium silicate glass-water reactions: mechanisms

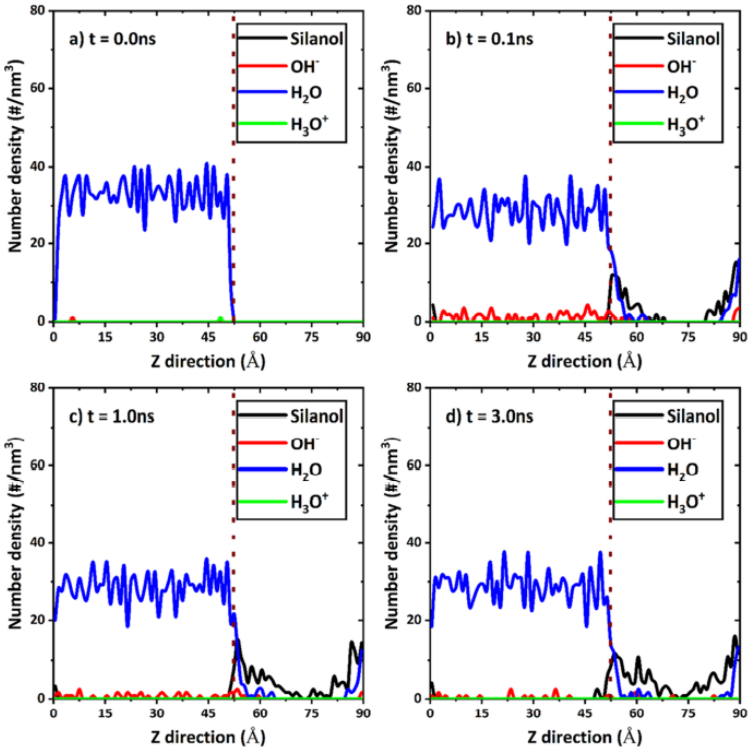

- ReaxFF based MD simulations up to 3 ns
- $77SiO_2$-$22Na_2O$ glass

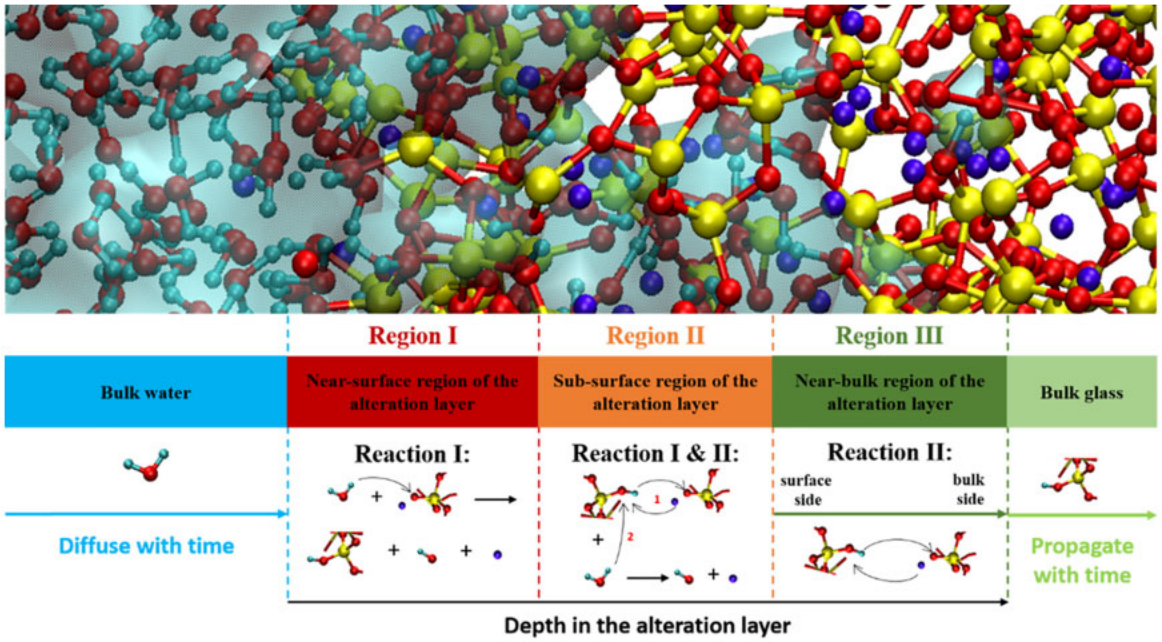

- Water react with the glass surface (NBO) through hydration reactions: Si-ONa + H_2O → Si-OH + Na^+ + OH^-
- Further reaction mainly through proton transfer deeper into the glass (possible ion-exchange).

Deng et al. J. Phys. Chem. 123(2019)21538

Ion-exchange reactions in Na Silicate glasses

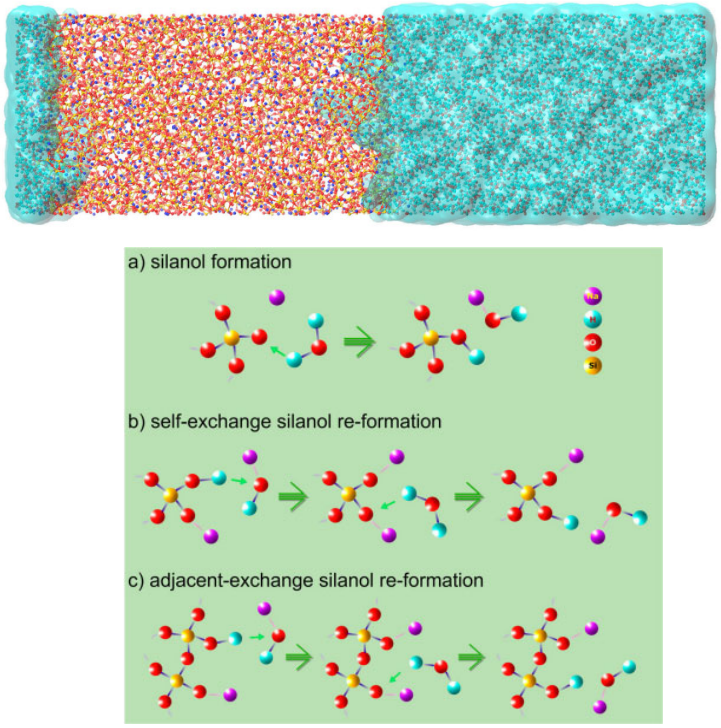

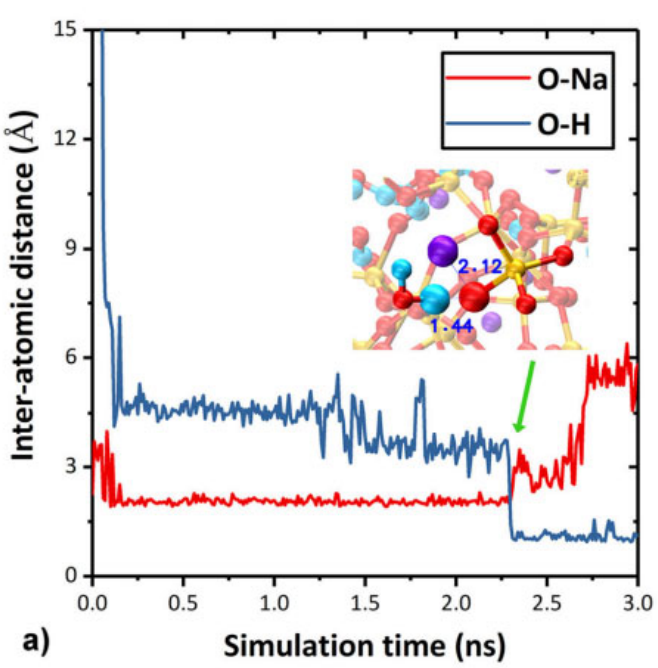

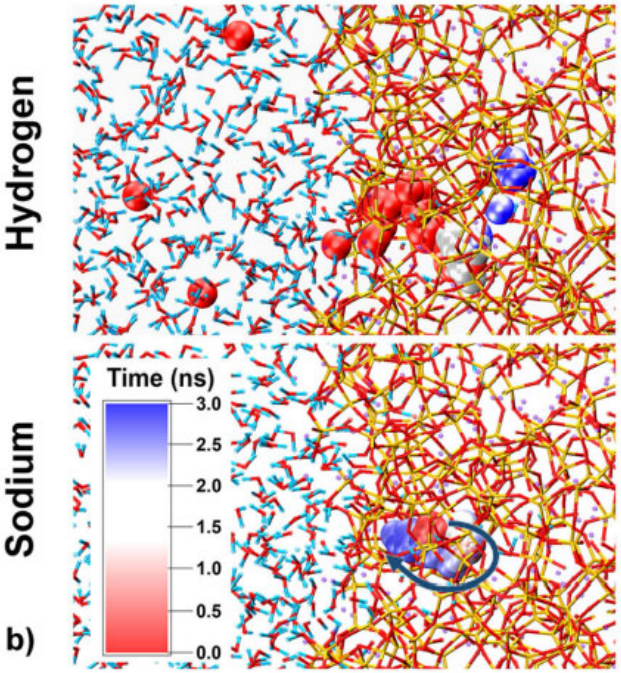

- ReaxFF based MD simulations with 0.1fs time step
- $77SiO_2$-$23Na_2O$ glass
- 300K and 450K simulations
- Direct observation of H^+/Na^+ ion-exchange process

Deng et al. npj Mater. Degrad. 1(2021)15

Silica gel structure generation from bulk glass structure

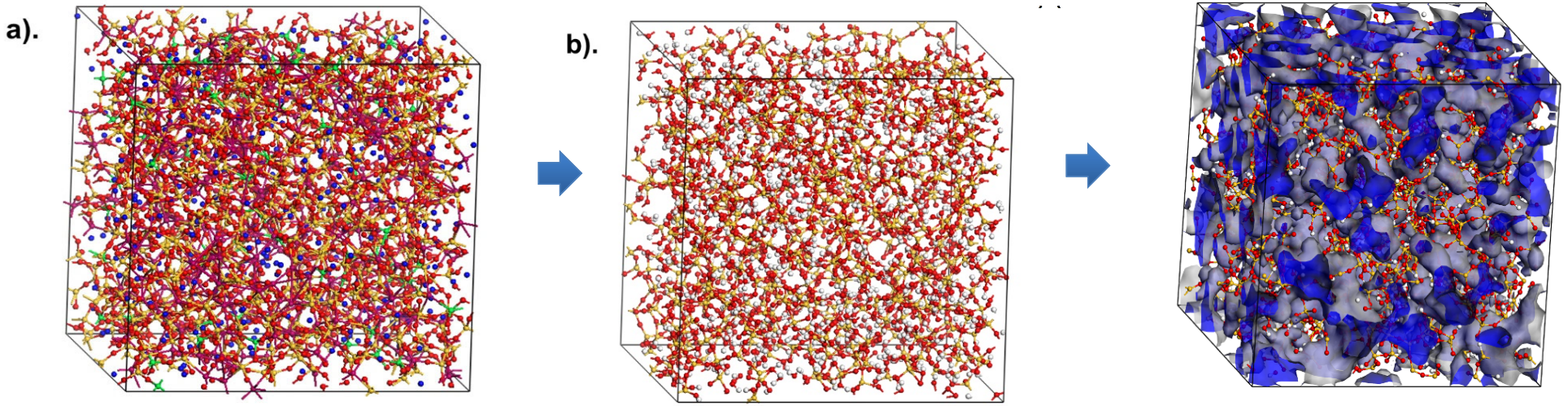

Bulk glass

Porous glass

Gel structure

- Two ways to generate gel layer structures: from preferential dissolution of ISG bulk glass structure
- From vacancy defect formation from dense silica
- Effect of formation method on atomic and microstructures evaluated. Water diffusion in the two structures examined.

Rimsza and Du, NPJ Mater. Degrad. 2018

Silica gel structure generation MD from dense silica

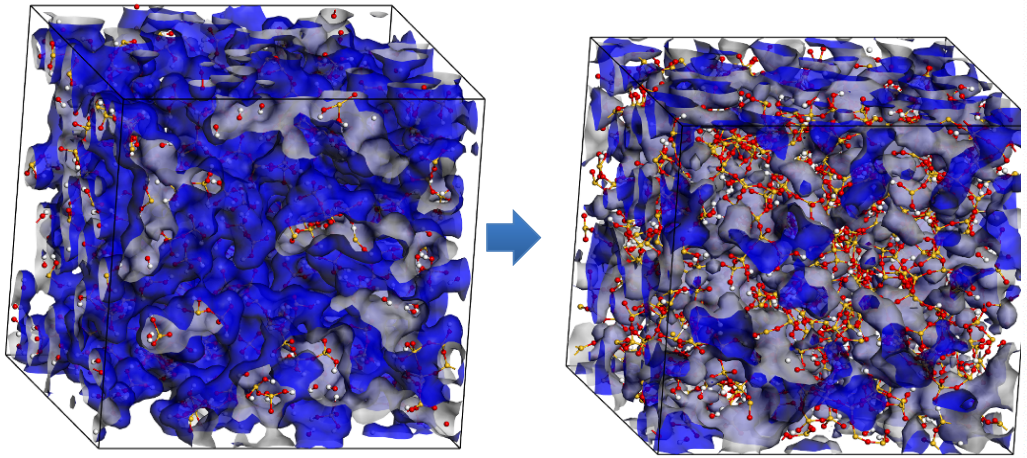

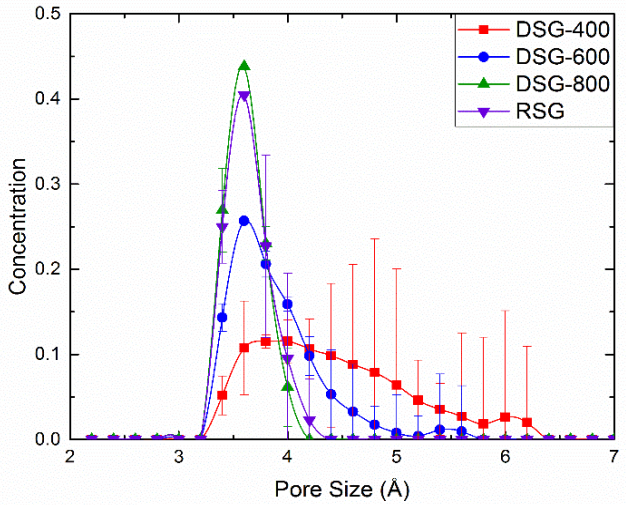

- Gel structure from dense silica with different porosity with ReaxFF based MD
- Si4+ were randomly removed and replaced by H+, e.g. hydrogarnet defect formation.
- DSG-600 and RSG (from ISG) show similar ring and pore size distributions

Rimsza and Du, NPJ Mater. Degrada. 2018

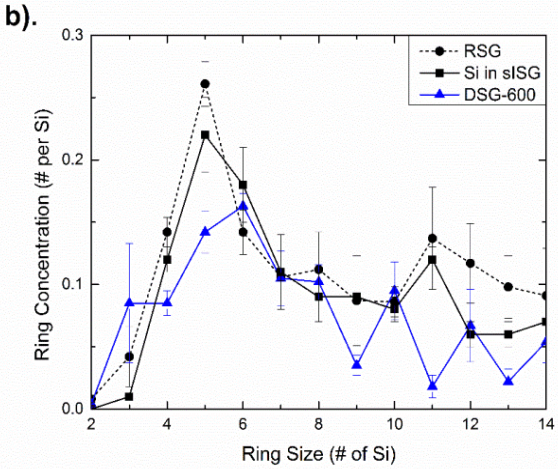

Water diffusions in porous gel structures

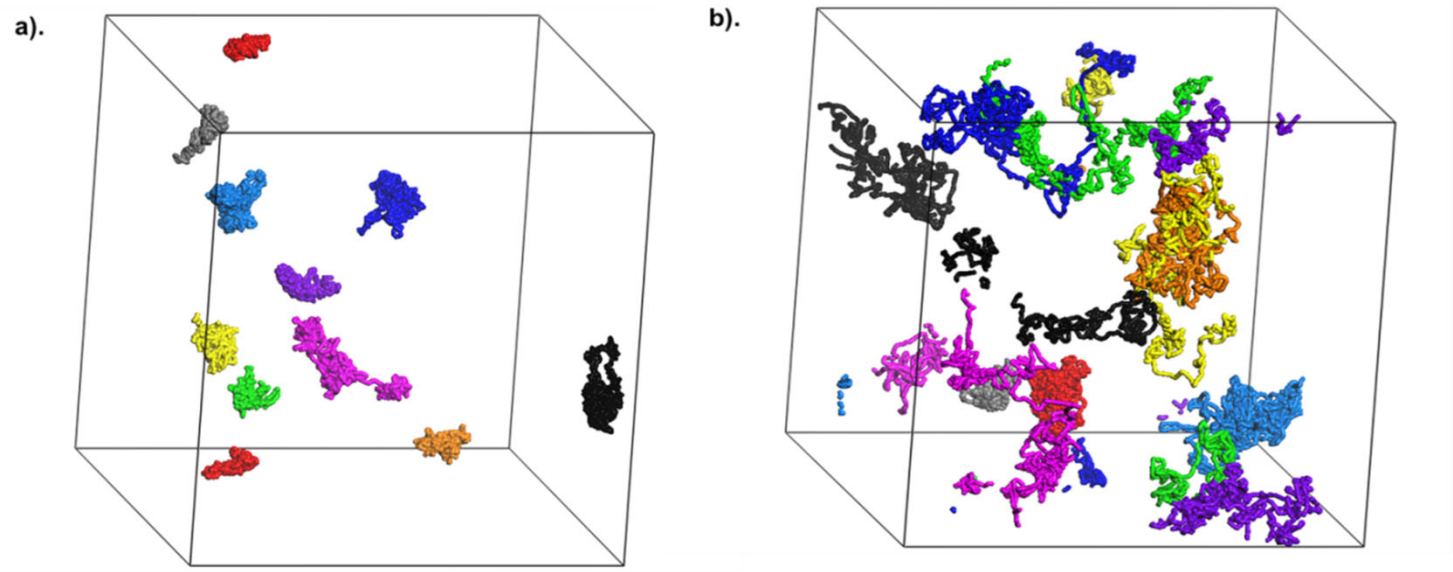

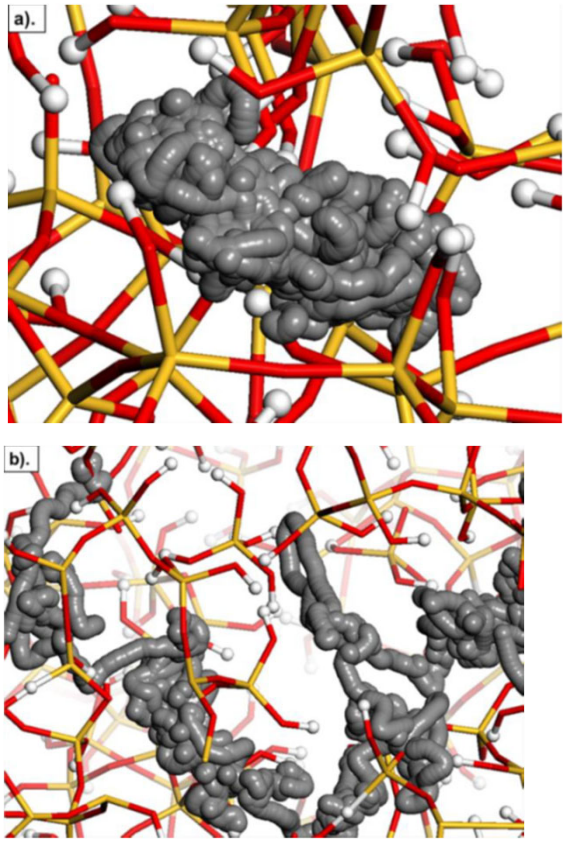

RSG (from ISG)

DSG-600 (from bulk silica)

- Similar pore size distribution and porosity but different diffusion behaviors.
- Remnant gel structures need further corrosion for water transport.

Rimsza and Du, NPJ Mater. Degrada. 2018

Diffusivity of water in confined geometry

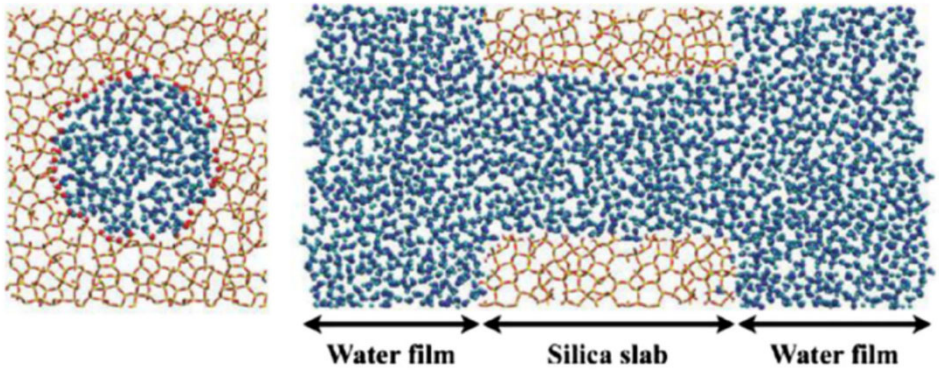

I. Bourg, JPCC 116 (2012) 11556

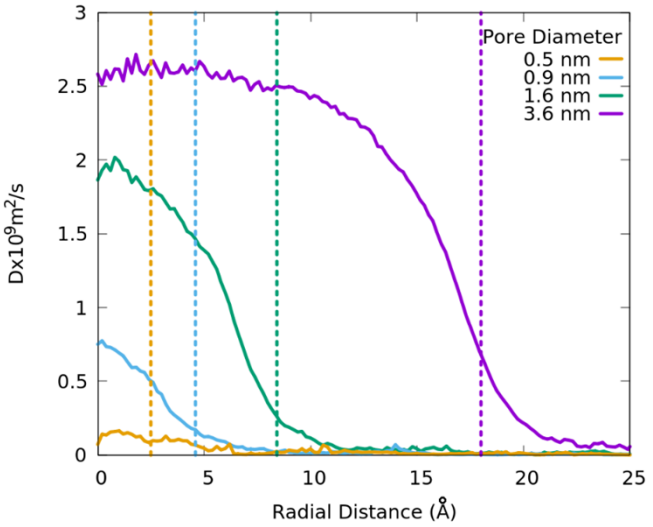

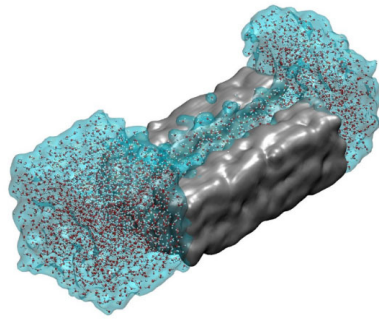

- Pore size determines the diffusivity at the center – larger pores attain unrestricted water diffusion at the pore center
- Diffusion in the hydrogen bonded network at the wall is always lower (under all confinements)

Colin et al, J Phys Chem C 2018
Gin et. al Nature Comm. 2019

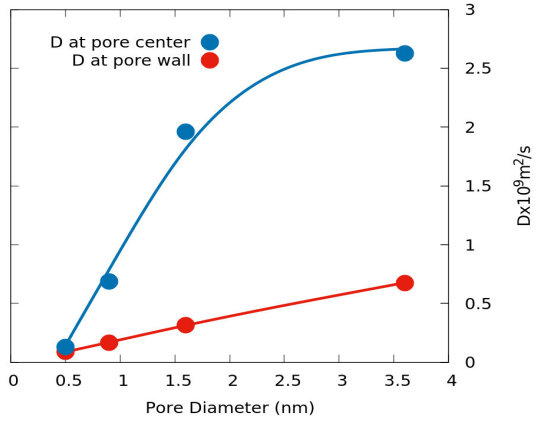

Properties of $CaO\text{-}Al_2O_3\text{-}SiO_2$ porous gel structures

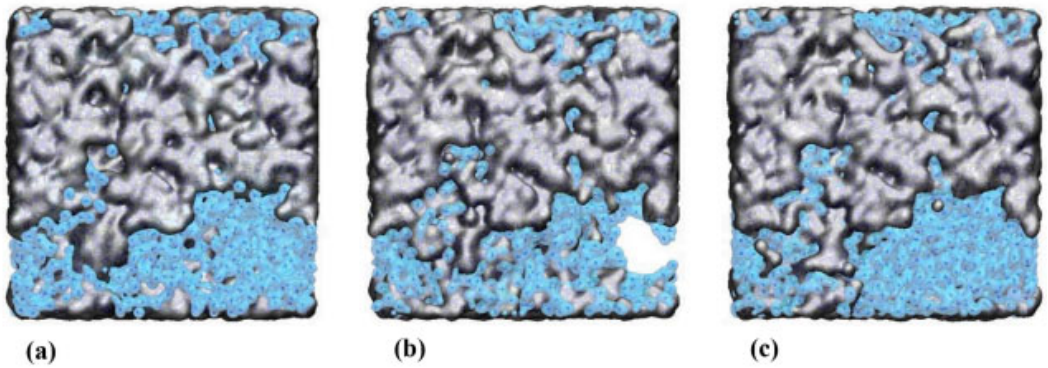

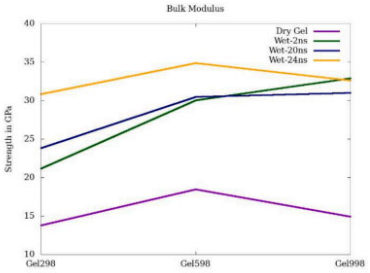

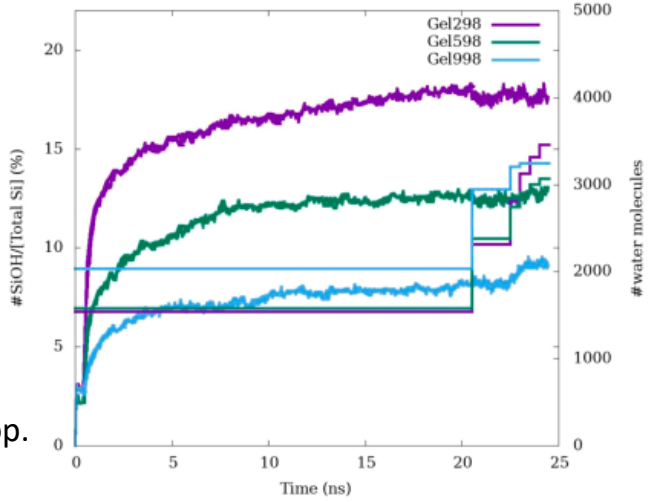

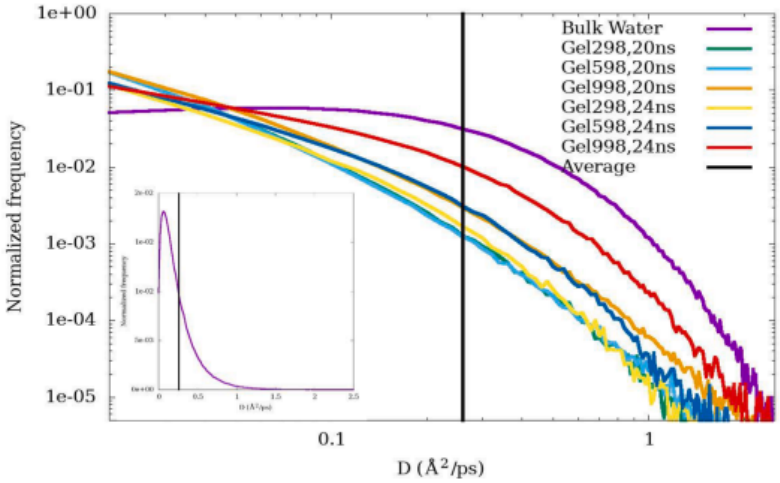

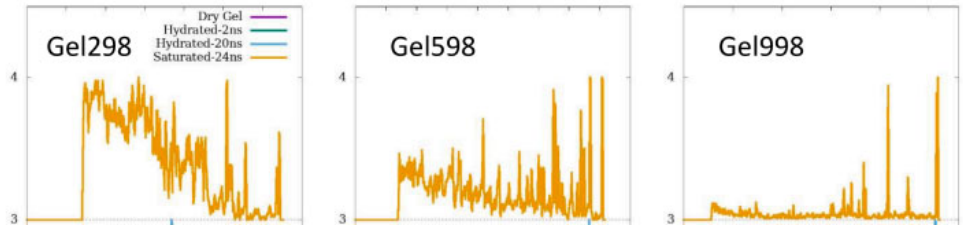

- DCRP reactive potential
- Up to 24 ns simulations
- Diffusion, mechanical prop.

Mahadevan, Du, JNCS 621(2023)122604

QSPR analysis of glass corrosion rate based on MD

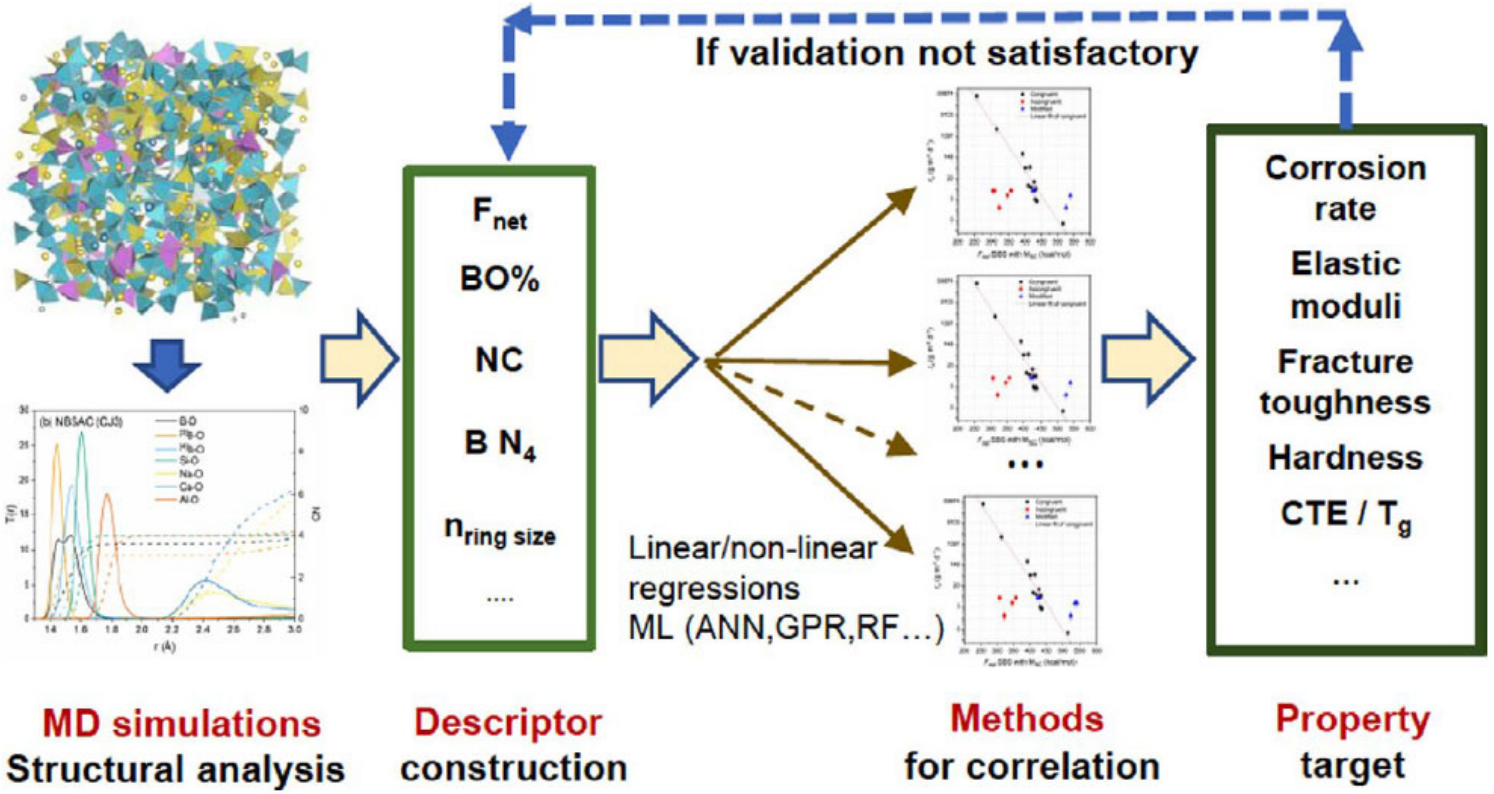

Du et al. J. Am. Ceram. Soc. 104(2021)4445

MD based QSPR analysis of properties of ISG+ZrO_2 glass

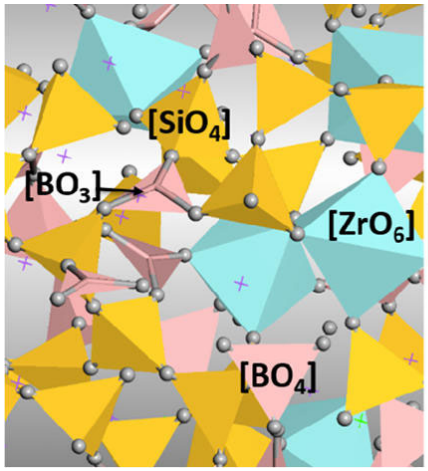

QSPR

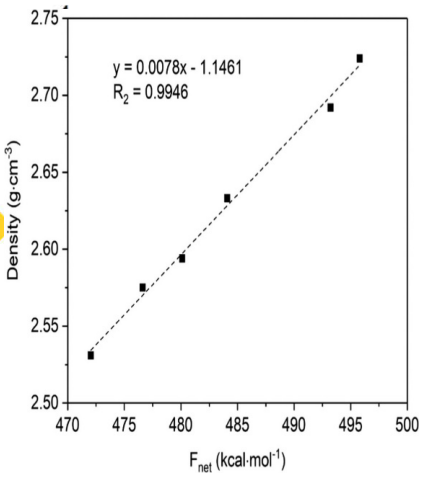

Density

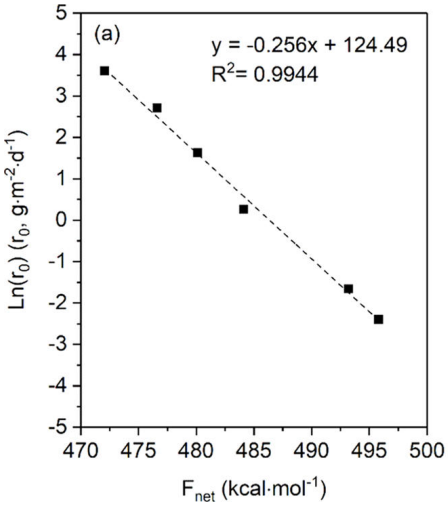

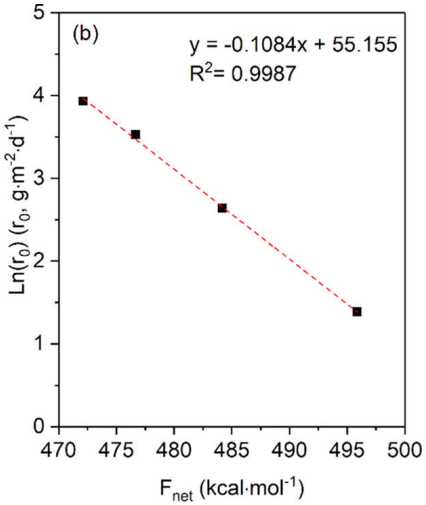

Initial dissolution rate r0

$(61 - x)SiO_2 \cdot xZrO_2 \cdot 17B_2O_3 \cdot 18Na_2O \cdot 4CaO$ x=0-8 mol%

Two sets of experimental measurements for forward rate (r0) available:

- Cailleteau et al. 90 °C in buffered solution (pH=6.9) without agitation
- Bergeron et al. 90 °C single pass flow through measurement
- Flow through measurements gave corrosion rate an order of magnitude higher for high ZrO_2 composition
- QSPR analysis provide excellent correlation of both sets of data: consistency of experimental data set

Lu, Deng, Gin, Du, J. Phys. Chem. B 123 (2019) 1412

UNT
UNIVERSITY OF NORTH TEXAS
EST. 1890

Structures of aluminosilicate and borosilicate glasses from MD

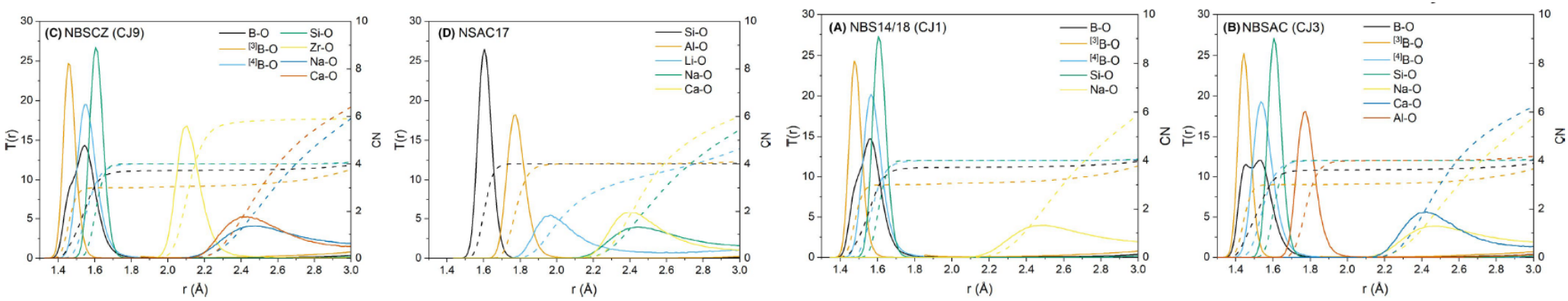

Glass	N_4 (%)				Oxygen speciation (%)			Ring size	
	YDBX[63,64]	Modified Bernstein[65]	MD	Exp.[18]	NBO	BO	TBO	Average size	>6, %
NBS14/18	73.5	65.8	70.2 ± 0.3	66	2.6 ± 0.1	96.4 ± 0.2	1.0 ± 0.1	7.28 ± 0.02	64.7 ± 0.6
NBSA	55.0	54.6	57.9 ± 0.3	48	1.8 ± 0.0	96.0 ± 0.1	2.3 ± 0.1	7.23 ± 0.02	63.9 ± 0.8
NBSAC	61.5	54.5	59.3 ± 0.5	53	5.9 ± 0.2	93.2 ± 0.4	0.9 ± 0.2	7.54 ± 0.04	66.7 ± 1.4
NBSACZ	62.3	52.9	61.3 ± 1.1	48	4.9 ± 0.2	93.3 ± 0.2	1.8 ± 0.1	7.40 ± 0.04	64.7 ± 0.6
NBSAZ	44.1	53.0	52.6 ± 0.8	41	1.6 ± 0.1	95.6 ± 0.3	2.8 ± 0.2	7.21 ± 0.04	63.6 ± 0.5
NBSC	73.5	69.3	70.6 ± 0.7	66	8.1 ± 0.1	91.7 ± 0.1	0.3 ± 0.1	7.63 ± 0.01	67.2 ± 0.5
NBSCZ	73.5	60.7	71.1 ± 1.0	63	6.5 ± 0.2	92.7 ± 0.3	0.8 ± 0.1	7.43 ± 0.05	65.0 ± 1.1
NBS12/28	41.8	56.1	42.6 ± 0.5	43	1.0 ± 0.1	97.8 ± 0.2	1.2 ± 0.1	7.97 ± 0.05	74.8 ± 0.8

Correlation of initial dissolution rate with F_{net}

Fnet: regular definition
R^2=88.8%

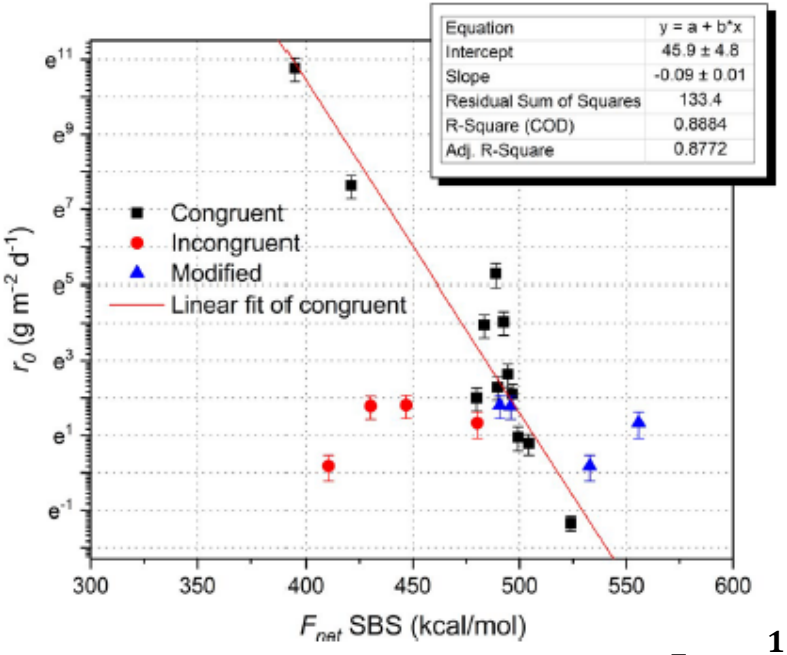

Fnet: modified definition
R^2=94.4%

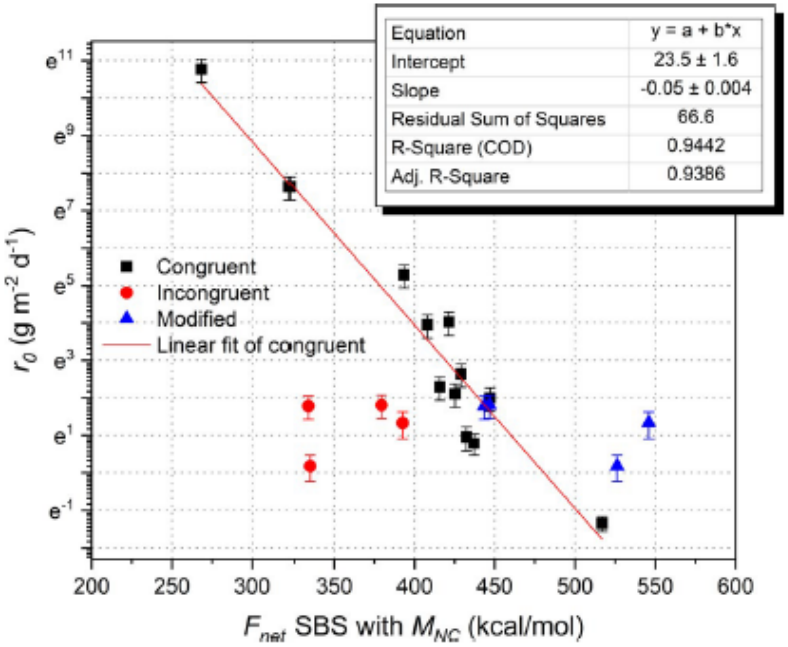

$$F_{net} = \frac{1}{N} \sum_{X}^{cations} n_X \cdot CN_{XO} \cdot SBS_{XO} \cdot m_X$$

Modifying the descriptor by introducing network connectivity improves the fitting.

Du et al. J. Am. Ceram. Soc. 104(2021)4445

Using structural features as descripts

BO percentage
R^2=56.3%

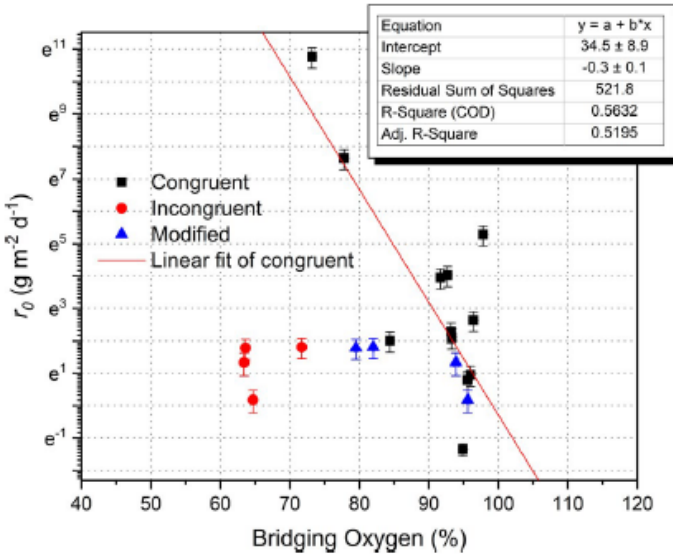

FIGURE 6 Correlation between initial dissolution rate r_0 (g m^{-2} day^{-1}) and percentage of bridging oxygen (BO%)

Average network connectivity
R^2=88.4%

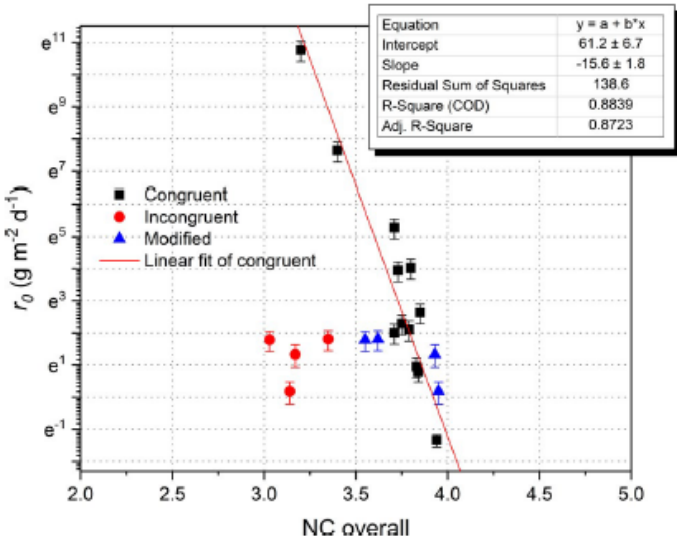

FIGURE 7 Correlation between initial dissolution rate r_0 (g m^{-2} day^{-1}) and overall network connectivity (NC), where Si, Al, B, and Zr are considered as network formers

Average ring size
R^2=90.3%

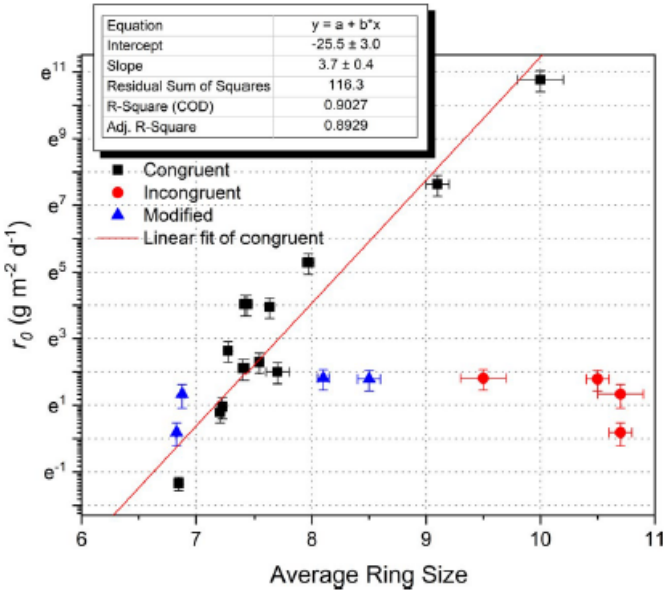

FIGURE 8 Correlation between r_0 (g m^{-2} day^{-1}) and average ring size

Du et al. J. Am. Ceram. Soc. 104(2021)4445

Correlation best the best descriptors

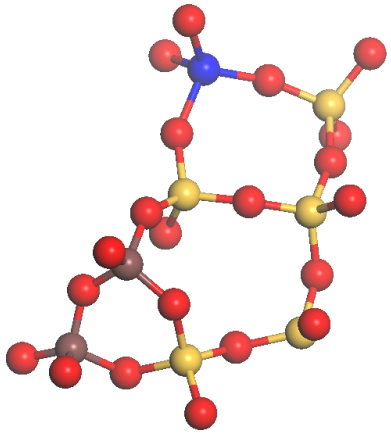

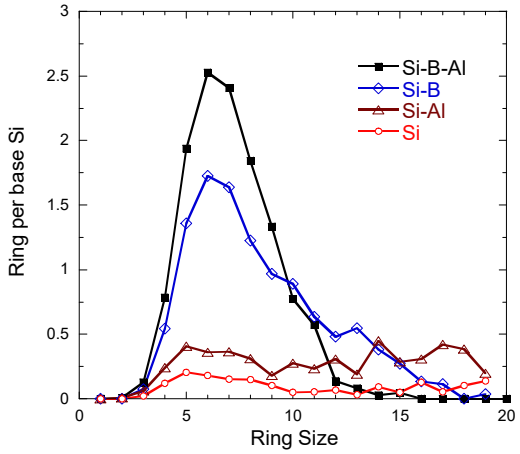

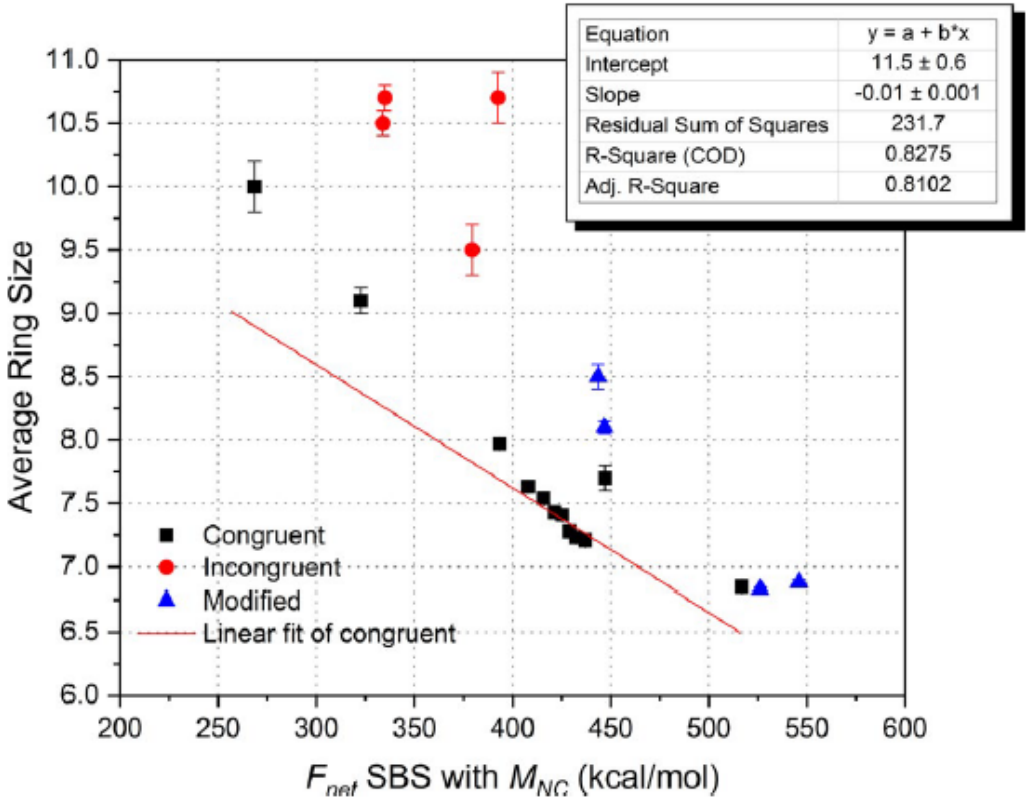

- Two best descriptors for initial dissolution rates are average ring size and F_{net} are linearly correlated
- Incongruent dissolution samples need to be modeled based on the modified composition
- Residual rate correlation possible by introducing descriptors with gel characteristics

Du et al. J. Am. Ceram. Soc. 104(2021)4445

Correlation of borosilicate glass corrosion rate with TCT

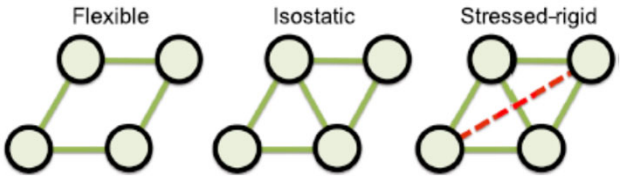

Bauchy, ComputMSE 2018

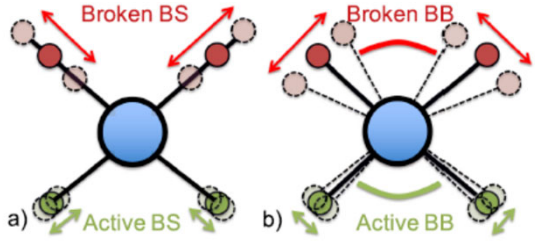

	BS	BB
Si	4	5
B^{III}	3	3
B^{IV}	4	0
Al	4	5
Na	1	0
Ca	2	0
BO	0	1
NBO	0	0

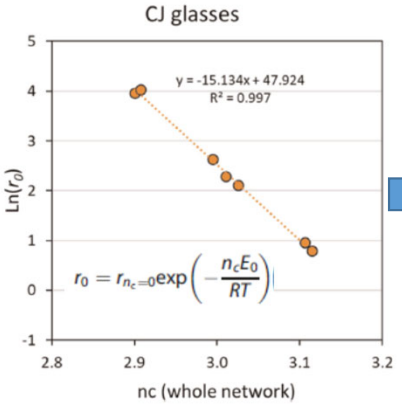

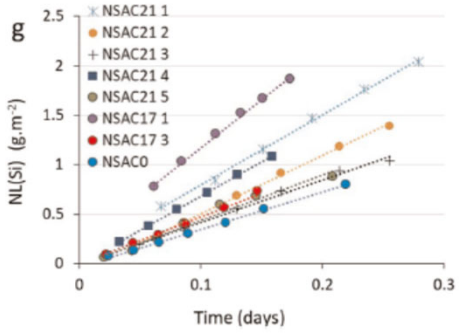

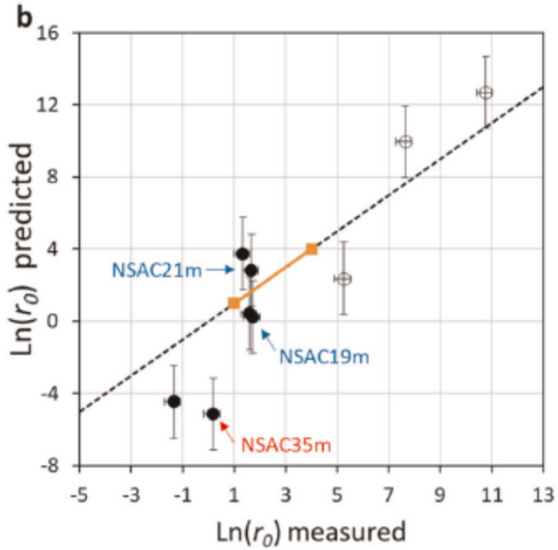

- Topological constraint theory (TCT) is shown to be capable to correlate with initial corrosion rate (r_0) for a wide range of borosilicate glasses
- Exceptions found in a few aluminosilicate glasses that have preferential leaching
- Correction of the composition can improve the correlation

Gin et al. npj Mater Degrad 2020

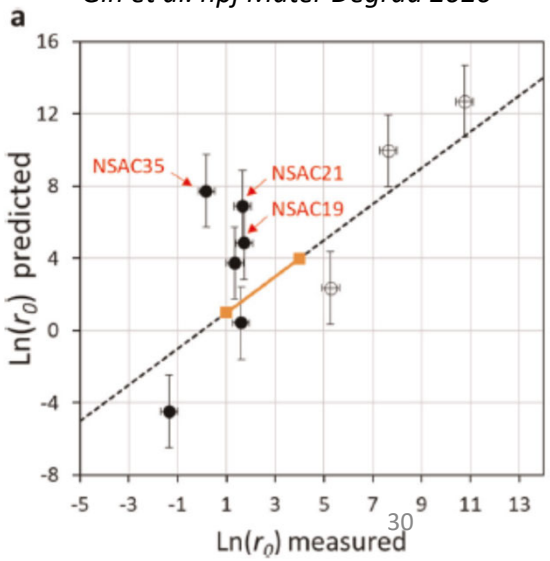

Predict dissolution rate from structure features from MD simulations

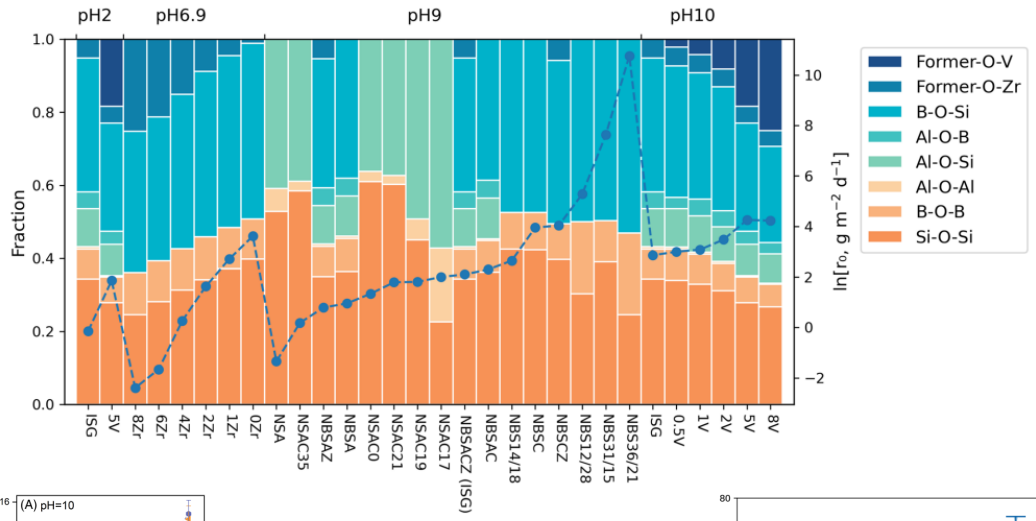

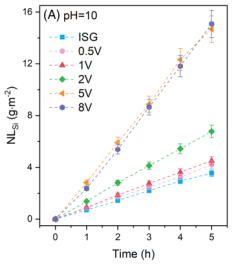

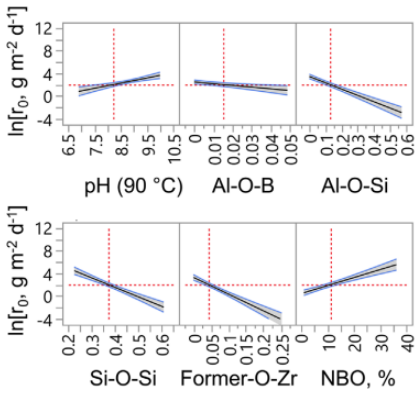

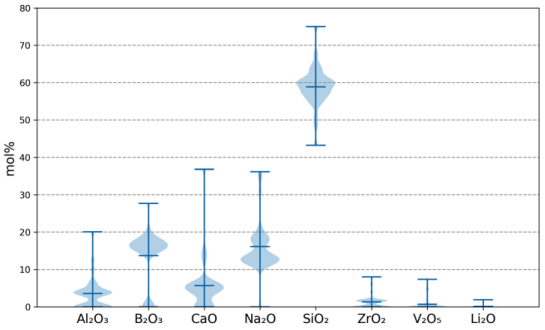

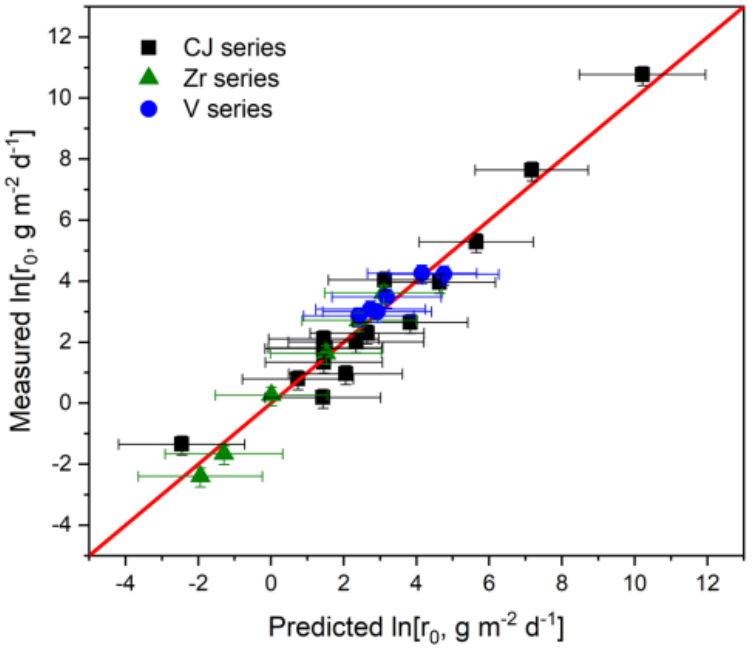

Predicting initial dissolution rates using structural features from molecular dynamics simulations

Xiaonan Lu[1] | Lu Deng[2] | Stéphane Gin[3] | Benjamin Parruzot[1] | Joelle T. Reiser[1] | Joseph V. Ryan[1] | John D. Vienna[1] | Jincheng Du[2]

Lu et al. JACerS 106(2022)1025

Monte Carlos simulations of glass corrosion

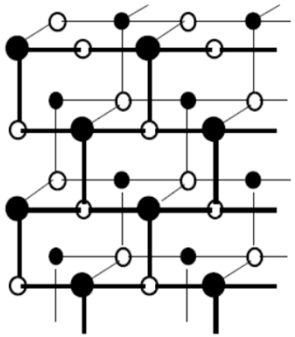

MC models rely on regular lattices to approximate glass structure

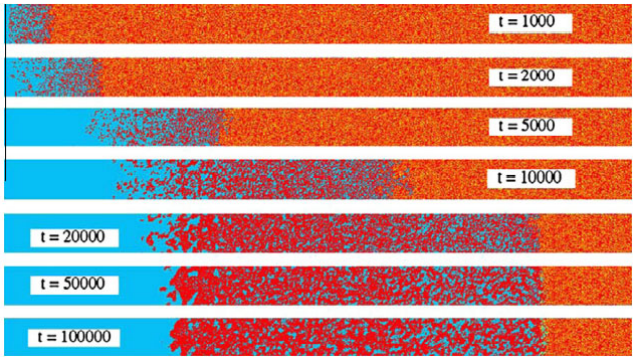

MC simulations of leaching of borosilicate glass

Devreux et al., JNCS 343(2004)13

MC simulation based on structure models from MD

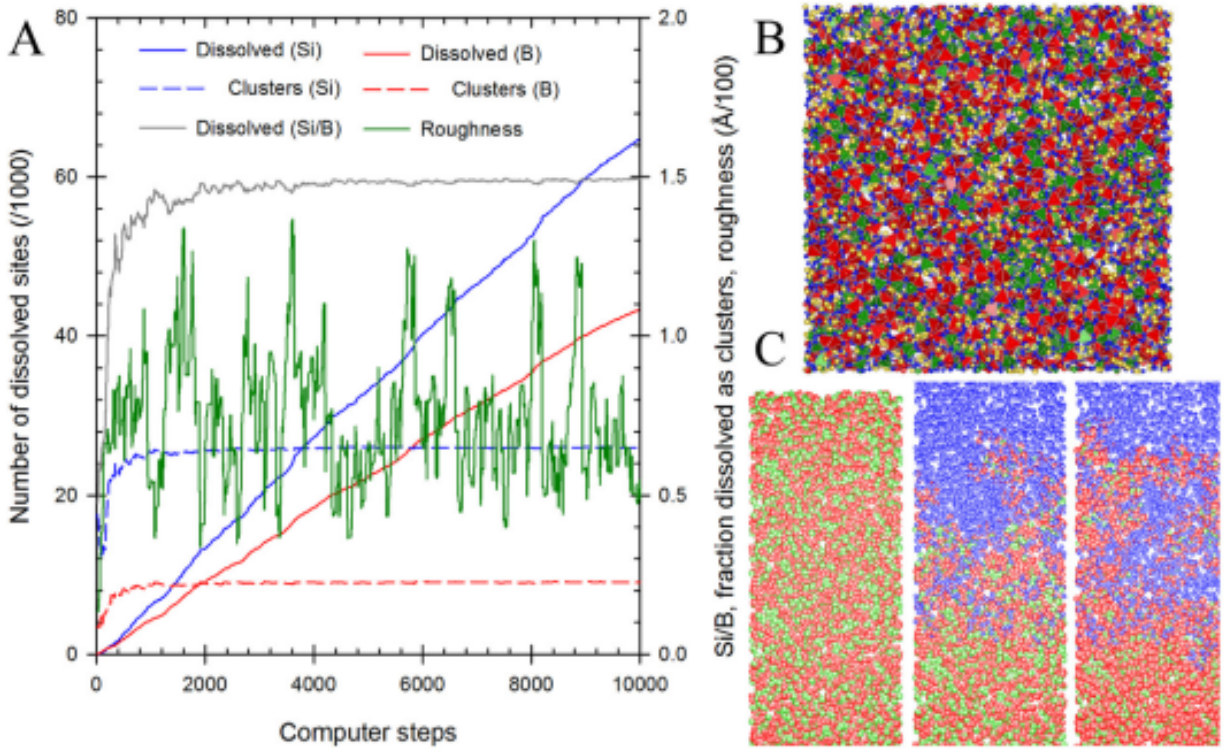

42.9 SiO_2–14.3 B_2O_3–42.9 Na_2O

Keresit & Du, *J. Non-Cryst. Solids,* 522(2019)119601

Monte Carlos simulations of sodium borosilicate glass corrosion

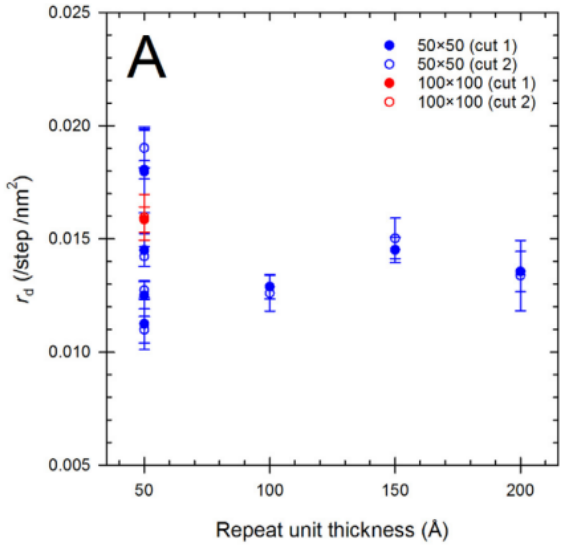

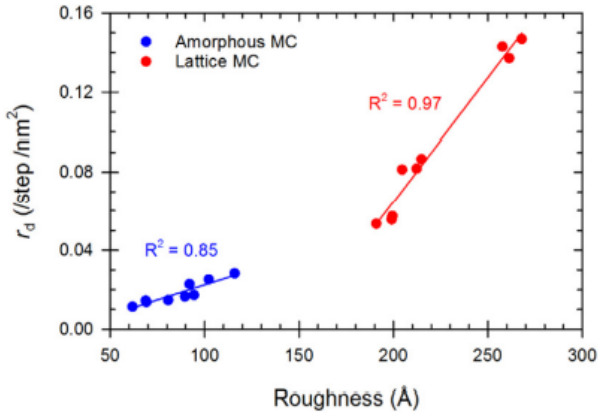

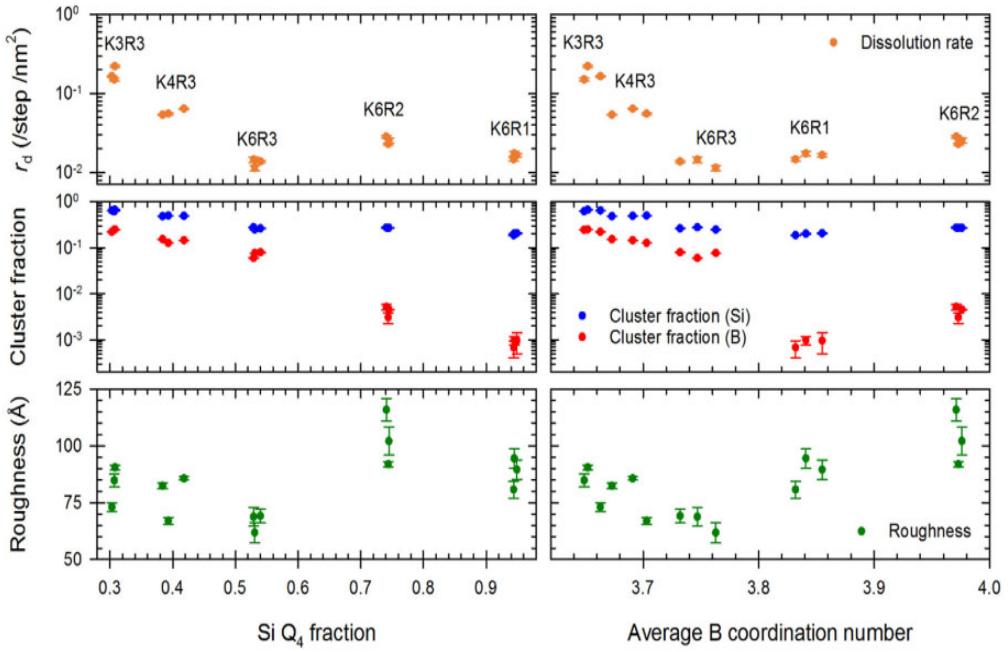

- MC based on glass structure generated from MD
- Effect of repeating unit thickness on dissolution rate investigated
- Dissolution rate and surface roughness studied as a function of glass composition
- Surface roughness a lot lower than regular lattice models

Keresit & Du, *J. Non-Cryst. Solids,* 522(2019)119601

Understand of Glass Corrosion with MD based Simulations

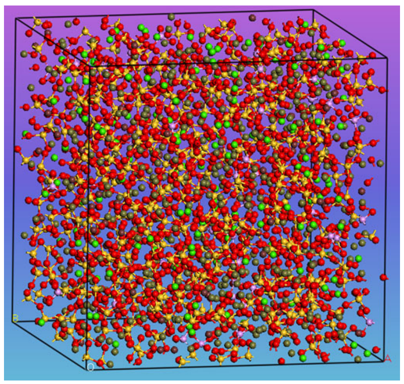

Glass structure from MD simulations & characterizations

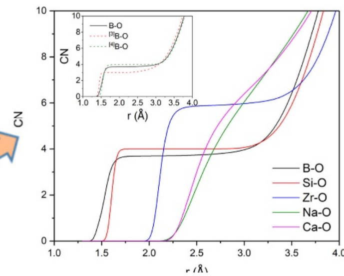

QSPR analysis

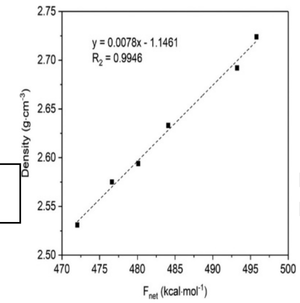

Lu et al. npj Mater. Degrad 2019
Du et al. J. Am Ceram. Soc 2021

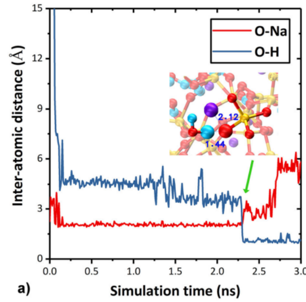

Reaction mechanism, interfacial structure/evolution

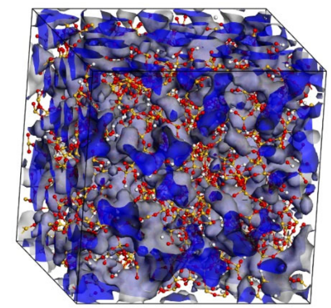

Rimsza and Du, JPCC 2018
Deng et al, JPCC 2018
Deng et al. npj Mater Degra 2019

Gel structure and transport

MC simulations of glass corrosion

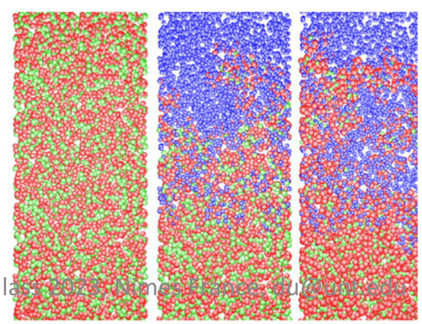

Kerisit, Du, JNCS 2019
Kerisit, Mahadevan, Du, JNCS 2021

Glass dissolution mechanism & corrosion rate prediction

UNT UNIVERSITY OF NORTH TEXAS EST. 1890

Conclusions and outlook

- Atomistic simulations and particularly classical MD simulations are highly valuable tools to understand nuclear waste glass structures and glass-water interactions.
- Development of interatomic potentials (reactive and non-reactive) are needed to enable some of these simulations.
- Complex nuclear waste glass structures, including redox effect and phase separation, can be studied as a function of glass composition.
- Interfacial structures of water/glasses are modeld to understand the corrosion gel structures. Diffusion and other properties can be investigated in the bulk, the gel and the interface.
- MD based QSPR approach valuable for corrosion rate and other property predictions
- Machine learning has been increasing used with the MD data or other structure features from glasses.

Acknowledgements:

Collaborators:

John Vienna, Joe Ryan, Sebastien Kerisit, Brian Riley (PNNL)

Stephane Gin, Jean-Marc Delaye (CEA)

John McCloy (Washington State U)

Ashutosh Goel (Rutgers U)

Delia Brauer (University of Jena)

Daniel R. Neuville (CNRS)

Jerry Frankel (Ohio State)

Seong Kim (Penn State)

Qiang Fu, Ying Shi (Corning Inc.)

Shingo Urata, Madoka Ono (AGC)

Graduate students/postdocs:

Lu Deng, TS Mahadevan, Xiaonan Lu, Jessica Rimsza, Wei Sun, Wenqing Xie, Jayani Kalahe, Mengguo Ren

Funding support:

DOE NEUP DOE EFRC Waste PD

NSF DMR Ceramics, AGC, Corning Inc.

Computer Time Support:

TACC, UNT Talon3, Cruntch3/4

Functional Glasses and Materials Modeling Laboratory

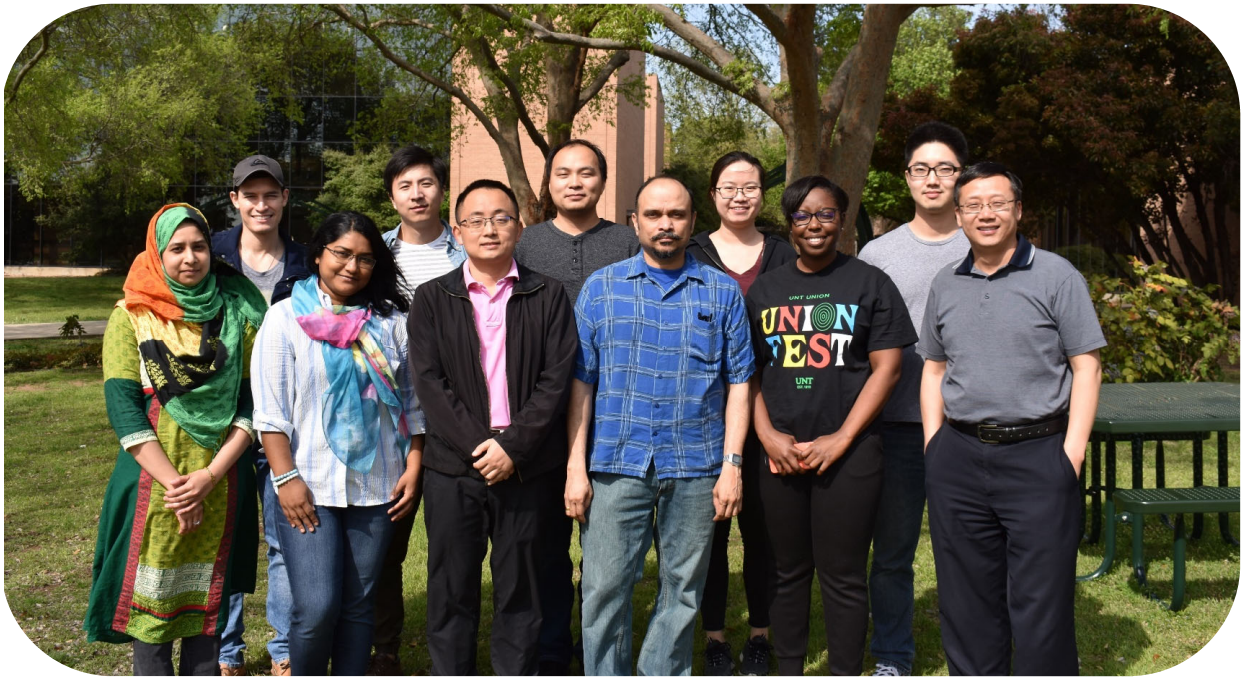

Thank you!

ICG
International Commission on Glass

TC27: Atomistic Simulation

UNT
UNIVERSITY OF NORTH TEXAS
EST. 1890